ARCTIC CURVES OF THE OCTAHEDRON EQUATION

PHILIPPE DI FRANCESCO AND RODRIGO SOTO-GARRIDO

ABSTRACT. We study the octahedron relation (also known as the A_∞ T-system), obeyed in particular by the partition function for dimer coverings of the Aztec Diamond graph. For a suitable class of doubly periodic initial conditions, we find exact solutions with a particularly simple factorized form. For these, we show that the density function that measures the average dimer occupation of a face of the Aztec graph, obeys a system of linear recursion relations with periodic coefficients. This allows us to explore the thermodynamic limit of the corresponding dimer models and to derive exact "arctic" curves separating the various phases of the system.

CONTENTS

Date: February 20, 2014.

1. Introduction

The octahedron recurrence is a system of non-linear equations describing the evolution of a quantity $T_{i,j,k}$, $i, j, k \in \mathbb{Z}$ corresponding to discrete space (i, j) and time k. This equation first arose in the context of integrable quantum spin chains with a Lie group symmetry [30, 31], and is obeyed by the corresponding quantum transfer matrices. In this language, the octahedron equation corresponds to the so-called T-system (for A_∞). In this formulation, the indices i, k, j respectively stand for representation indices, and a discrete spectral parameter. The A-type T-systems have remarkable properties, depending on the choice of boundary conditions, such as discrete integrability [13], and periodicity properties [22, 15] as well as the positive Laurent property (solutions are Laurent polynomials of the initial data with non-negative integer coefficients) in relation to cluster algebras [9].

This equation or some restrictions thereof appear to be central in a number of combinatorial constructs, such as the Desnanot-Jacobi relation between minors of a given matrix and the Dodgson condensation of determinants [16], the lambda-determinant and alternating sign matrices [4, 36, 10], the puzzles for computing Littlewood-Richardson coefficients [29], various generalizations of Coxeter-Conway frieze patterns [8, 1, 3], and cluster algebra [12] to name a few.

A great progress in understanding the combinatorics of the octahedron equation was due to Speyer [37], who worked out the general solution in terms of a dimer model on a graph, also equivalent to the domino tiling problem of the Aztec diamond [17]. This establishes the connection between a general set of solutions of the octahedron equation with given initial data, and the partition functions of statistical lattice models of dimers, whose local Boltzmann weights are defined in terms of these data. This was recently extended to more general initial conditions, giving rise to dimer models on specific graphs [11]. Note also that a large class of dimer models on periodic graphs was recently shown to have both integrable and cluster algebra structures as well [21]. Finally, the study of the so-called pentagram map, an integrable dynamical system on polygons of projective plane displayed intriguing connections [20] with solutions of the octahedron equation with special periodic initial conditions. An analogous connection exists for the generalization to higher pentagram maps [19, 15, 25].

Dimer models were the subject of a lot of attention, starting with the so-called arctic circle theorem for the domino tilings of large Aztec diamonds [24], and later culminating in the global understanding of the arctic curve phenomenon in the continuum limit [26] [27], where the phase diagram of the model was shown to exhibit separations between frozen, disordered, and liquid phases. Analogous phenomena were observed for groves [32], for the double-dimer model connected to the hexahedron recurrence [28] and for the six-vertex model [7].

In the present paper, we revisit the case of domino tilings/dimer coverings of the Aztec diamond, from the point of view of Speyer's general solution of the octahedron relation. We

construct explicit exact solutions of the octahedron equation for an infinite class of initial data with special periodicity conditions. These in turn are partition functions for dimer models with periodic weights. For these solutions, we show that a certain local density function, that measures the average dimer occupation of a face of the Aztec graph, obeys a system of linear recursion relations with *periodic* coefficients. This allows to compute the density generating function explicitly in the form of a rational fraction. Following [33, 34, 35, 28], the study of the denominator of this function allows to explore the singularity structure of the dimer models in the thermodynamic limit of large size, and to confirm their phase structure, displaying frozen, disordered and facet-like phases separated by generalized "arctic" curves.

The paper is organized as follows.

In Section 2, we recall facts on the A_∞ T-system/octahedron equation and its initial conditions, as well as its solution as a dimer partition function on the Aztec graph. As a preparatory exercise, we compute the density generating function for the uniform initial data and show how to extract the arctic circle form the explicit solution.

In Section 3, we study in detail 2×2 periodic initial data, for which the T-system is wrapped on the torus generated by $(2, 0)$ and $(0, 2)$ in $\mathbb{Z}^2$. The density generating function is found to solve a linear 4×4 system, whose explicit solution displays two disconnected pieces of "arctic" curve, separating the dimer configurations in the thermodynamic limit into three phases: (i) four frozen corners with a single dominant configuration induced by the geometry of corners; (ii) a disordered "temperate region" analog to the inside of the arctic circle, and (iii) a new "facet"-like central phase, where the configurations are pinned to the sub-lattice corresponding to the faces with the smallest Boltzmann weight.

Section 4 is devoted to the class of so-called m-toroidal boundary conditions. We first construct the explicit solution to the T-system, and then show that it leads to linear systems for the density function with *triply* periodic coefficients in $\mathbb{Z}^3$. As a result, the density generating function is shown to satisfy a $4m \times 4m$ linear system, whose determinant captures the information on the generalized arctic curves that separate different phases. For this model, we find generically the same phases: (i) frozen corners; (ii) disordered region; (iii) in general $m - 1$ facets whose position and size vary with the initial data.

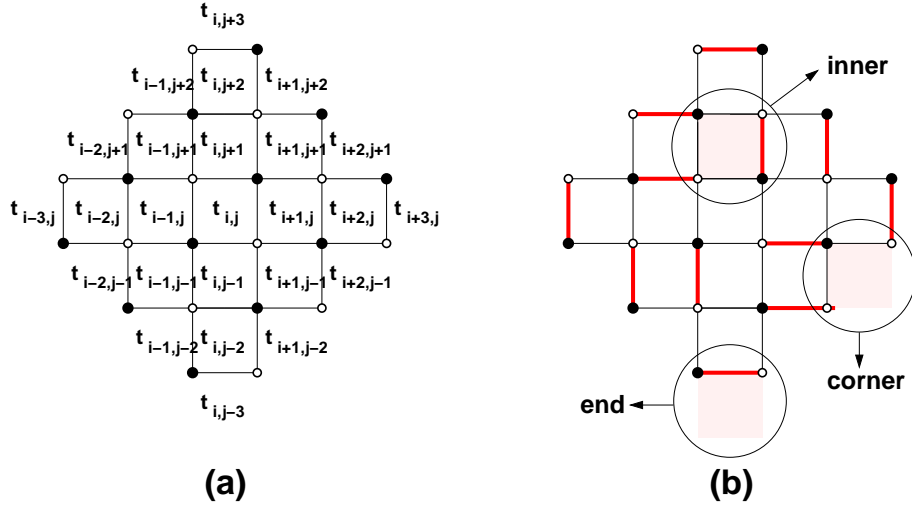We gather a few concluding remarks in Section 5.

FIGURE 1. A typical Aztec diamond graph $\mathcal{A}_{i,j,k}$ for $k = 4$ (a) with its face labeling, and a sample dimer configuration on $\mathcal{A}_{i,j,k}$ (b). We have shaded the three types of faces: inner, corner, end, respectively adjacent to 4,2,1 edges of $\mathcal{A}_{i,j,k}$.

2. T-SYSTEM, DIMERS AND ARCTIC CURVE

2.1. **The A_∞ T-system.** The unrestricted A_∞ T-system (from now on we will drop the A_∞ label), also known as the octahedron recurrence, is given by the following difference equation (for a detailed review of the T-system see [31]):

$$(2.1) \qquad T_{i,j,k+1}T_{i,j,k-1} = T_{i+1,j,k}T_{i-1,j,k} + T_{i,j+1,k}T_{i,j-1,k}$$

where $i, j, k \in \mathbb{Z}$ and $T_{i,j,k} \in \mathbb{R}$. Notice that the system conserves parity $i + j + k = 0, 1$ mod 2. Let us fix it to 1 throughout the paper. One way to think about the T-system is to consider i, j as labeling points on the square lattice and k as a discrete time (as the vertical axis of a cubic lattice). In this sense the T-system (2.1) describes the evolution in time of a given initial data (see Di Francesco [11]). In this paper we will work with a flat initial data, meaning that the value of the T variables is specified on the $(i, j, 0)$ and $(i, j, 1)$ planes, namely we fix:

$$(2.2) \qquad T_{i,j,i+j+1\,\mathrm{mod}\,2} = t_{i,j} \qquad (i, j \in \mathbb{Z})$$

In this paper, we consider the solution $T_{i,j,k}$ to the T-system (2.1) subject to various restrictions of the initial condition (2.2). These will be simply the result of imposing extra periodicity conditions on the initial data $t_{i,j}$, the simplest of which being the uniform case when all $t_{i,j} = 1$.

2.2. **Dimer formulation.** The solution $T_{i,j,k}$, for $i + j + k = 1$ mod 2, $i, j \in \mathbb{Z}$, $k \geq 0$, of the A_∞ T-system (2.1) with initial data (2.2) was identified as the partition function for domino tilings of the Aztec diamond, or dually to the dimer coverings of the Aztec diamond graph $\mathcal{A}_{i,j,k}$ [37, 11]. The graph $\mathcal{A}_{i,j,k}$ has vertices at points of the lattice $\mathbb{Z}^2$. Let us label the faces of $\mathbb{Z}^2$ by the coordinate (i, j) of their lower left corner vertex. Then $\mathcal{A}_{i,j,k}$ has faces (a, b) such that $|a - i| + |b - j| \leq k - 1$. Each such face receives the label $t_{a,b}$, the initial data assignment of the T-system. The edges of the graph are inherited from those of the underlying square lattice, however the boundary faces have only one or two adjacent edges depending on whether they are corner faces or end faces (see Fig. 1 for an illustration). The vertices of $\mathcal{A}_{i,j,k}$ are naturally bicolored black/white, according to the parity of $i + j = 0/1$ mod 2.

Definition 2.1. *The dimer model on $\mathcal{A}_{i,j,k}$ is defined as follows. The configurations of the model are matchings of pairs of vertices connected via an edge (dimers) such that any vertex of $\mathcal{A}_{i,j,k}$ belongs to exactly one dimer. Each configuration is weighted by a product over all faces (a, b) of $\mathcal{A}_{i,j,k}$ of local weights $w_{a,b}$. For any face (a, b) (including boundary faces) the weight is*

$$w_{a,b} = (t_{a,b})^{1-D_{a,b}}$$

where $D_{a,b} \in \{0, 1, 2\}$ is the total number of dimers occupying the edges of the square face. The partition function of the model is

$$Z_{i,j,k} = \sum_{\substack{\text{dimer} \\ \text{configurations}}} \prod_{\text{faces } (a,b)} w_{a,b}$$

The analysis of the present paper is based on the following main result:

Theorem 2.2. [37, 11] *The solution $T_{i,j,k}$, for $i + j + k = 1$ mod 2, $i, j \in \mathbb{Z}$, $k \geq 0$, of the A_∞ T-system (2.1) with initial data (2.2) is the partition function of the dimer model on $\mathcal{A}_{i,j,k}$, namely*

$$T_{i,j,k} = Z_{i,j,k}$$

2.2.1. *Density.* Consider the solution $T_{i,j,k}$ to the T-system with initial data (2.2). If we think of $T_{i,j,k}$ as a partition function, then the derivative $t_{\epsilon,\eta} \partial_{t_{\epsilon,\eta}} \mathrm{Log}\, T_{i,j,k}$ corresponds to some susceptibility or density, where $t_{\epsilon,\eta}$ acts as a source, here a magnetic field attached to dimers around the (ϵ, η) face. More precisely, we have

$$t_{\epsilon,\eta} \partial_{t_{\epsilon,\eta}} \mathrm{Log}\, T_{i,j,k} = \langle 1 - D_{\epsilon,\eta} \rangle \ ,$$

the statistical average of $1-$ the number of dimers surrounding the face (ϵ, η) within the set of dimer configurations on $\mathcal{A}_{i,j,k}$. Assume we further restrict the initial values to $t_{a,b} = t_{a,b}^*$, $a, b \in \mathbb{Z}$.

Definition 2.3. *We define the density function $\rho_{i,j,k}^{(\epsilon,\eta)}$ as:*

$$(2.3) \qquad \rho_{i,j,k}^{(\epsilon,\eta)} = t_{\epsilon,\eta}\, \frac{\partial}{\partial t_{\epsilon,\eta}} \mathrm{Log}\, T_{i,j,k} \Bigg|_{t_{a,b}=t_{a,b}^*}$$

We can easily derive a linear recurrence relation for $\rho_{i,j,k}^{(\epsilon,\eta)}$ by taking the derivative with respect to $t_{\epsilon,\eta}$ of the T-system relation (2.1). After some straightforward algebra we have:

$$(2.4) \qquad \rho_{i,j,k+1}^{(\epsilon,\eta)} + \rho_{i,j,k-1}^{(\epsilon,\eta)} = L_{i,j,k}(\rho_{i+1,j,k}^{(\epsilon,\eta)} + \rho_{i-1,j,k}^{(\epsilon,\eta)}) + R_{i,j,k}(\rho_{i,j+1,k}^{(\epsilon,\eta)} + \rho_{i,j-1,k}^{(\epsilon,\eta)})$$

where we used the notation:

$$(2.5) \qquad L_{i,j,k} = \frac{T_{i+1,j,k}T_{i-1,j,k}}{T_{i,j,k+1}T_{i,j,k-1}} \qquad \text{and} \qquad R_{i,j,k} = 1 - L_{i,j,k} = \frac{T_{i,j+1,k}T_{i,j-1,k}}{T_{i,j,k+1}T_{i,j,k-1}}$$

where $T_{i,j,k}$ are evaluated at $t_{a,b} = t_{a,b}^*$ for all $a, b \in \mathbb{Z}$. The recurrence relation is supplemented with the following initial data. Define $\varphi = (\epsilon + \eta + 1 \bmod 2)$. Then:

$$(2.6) \qquad \rho_{i,j,\varphi}^{(\epsilon,\eta)} = \delta_{i,\epsilon}\delta_{j,\eta} \qquad \rho_{i,j,1-\varphi}^{(\epsilon,\eta)} = 0 \qquad (i,j \in \mathbb{Z}; i+j+\epsilon+\eta = 0 \bmod 2)$$

Notice that in order to solve the recurrence relation for the density we need to know $L_{i,j,k}$ and $R_{i,j,k}$ appearing in (2.4). As we shall see below, the density $\rho_{i,j,k}^{(\epsilon,\eta)}$ is the variable that we will use to explore the behavior of the dimer model for large k.

2.3. **Arctic curve: the uniform case.** We start with the recurrence relation (2.4) for the uniform initial data:

$$(2.7) \qquad t_{i,j}^* = 1 \qquad (i,j \in \mathbb{Z})$$

In this case the solution for the T-system is simply given by $T_{i,j,k} = 2^{k(k-1)/2}$. The two ratios $L_{i,j,k}, R_{i,j,k}$ appearing in eq. (2.4) are equal to $1/2$.

To this uniform initial data we add up a source on the face $(\epsilon, \eta) = (0,0)$ or $(0,1)$, namely consider the densities $\rho_{i,j,k}^{(0,0)}, \rho_{i,j,k}^{(0,1)}$. Both densities obey the following recurrence relation:

$$(2.8) \qquad \rho_{i,j,k+1} + \rho_{i,j,k-1} = \frac{1}{2}(\rho_{i+1,j,k} + \rho_{i-1,j,k} + \rho_{i,j+1,k} + \rho_{i,j-1,k}) \qquad (i,j \in \mathbb{Z}; k \geq 1)$$

with initial data $\rho_{i,j,0}^{(0,0)} = 0$ and $\rho_{i,j,1}^{(0,0)} = \delta_{i,0}\delta_{j,0}$, while $\rho_{i,j,1}^{(0,1)} = 0$ and $\rho_{i,j,0}^{(0,1)} = \delta_{i,0}\delta_{j,0}$. Extending the validity of (2.8) to $k = 0$ allows to define

$$(2.9) \qquad \rho_{i,j,-1}^{(0,0)} = -\delta_{i,0}\delta_{j,0}$$

and

$$(2.10) \qquad \rho_{i,j,-1}^{(0,1)} = \frac{1}{2}(\delta_{i,-1} + \delta_{i,1})\delta_{j,0} + \frac{1}{2}(\delta_{j,-1} + \delta_{j,1})\delta_{i,0}$$

For $(\epsilon, \eta) = (0,0)$ or $(0,1)$, we define generating functions $\rho^{(\epsilon,\eta)}(x,y,z)$ as:

$$(2.11) \qquad \rho^{(\epsilon,\eta)}(x,y,z) = \sum_{i,j \in \mathbb{Z}, k \geq 0} \rho_{i,j,k}^{(\epsilon,\eta)} \, x^i \, y^j \, z^k$$

Multiplying both sides of (2.8) by $x^i y^j z^k$ and then summing over $i, j \in \mathbb{Z}, k \geq 0$ we get:

$$\sum_{i,j \in \mathbb{Z}, k \geq 0} (\rho_{i,j,k+1} + \rho_{i,j,k-1}) x^i y^j z^k = \frac{1}{2} \sum_{i,j \in \mathbb{Z}, k \geq 0} (\rho_{i+1,j,k} + \rho_{i-1,j,k} + \rho_{i,j+1,k} + \rho_{i,j-1,k}) x^i y^j z^k$$

for both density functions. Substituting the values of $\rho_{i,j,-1}$ from (2.9-2.10), we get:

$$(z^{-1} + z)\rho^{(0,0)}(x,y,z) = \frac{1}{2}(x^{-1} + x + y^{-1} + y)\rho^{(0,0)}(x,y,z) + 1$$

$$(z^{-1} + z)\rho^{(0,1)}(x,y,z) = \frac{1}{2}(x^{-1} + x + y^{-1} + y)\rho^{(0,1)}(x,y,z) + z^{-1} - \frac{1}{2}(x^{-1} + x + y^{-1} + y)$$

So the density generating functions for the uniform initial data are given by:

$$\rho^{(0,0)}(x,y,z) = \frac{z}{1 + z^2 - \frac{z}{2}(x^{-1} + x + y^{-1} + y)}$$

$$\rho^{(0,1)}(x,y,z) = \frac{1 - \frac{z}{2}(x^{-1} + x + y^{-1} + y)}{1 + z^2 - \frac{z}{2}(x^{-1} + x + y^{-1} + y)}$$

$$(2.12) \qquad\qquad = 1 - z\, \rho^{(0,0)}(x,y,z)(x,y,z)$$

Recall that $\rho_{i,j,k}^{(0,0)}$, $i + j + k = 1 \bmod 2$, is the average $\langle 1 - D_{0,0} \rangle_{i,j,k}$ in the dimer model on $\mathcal{A}_{i,j,k}$. It is the same as the average $\langle 1 - D_{-i,-j} \rangle_{0,0,k}$ (for $i + j$ even) in the dimer model on $\mathcal{A}_{0,0,k}$ when k is odd and as $\langle 1 - D_{-i,-j+1} \rangle_{0,1,k}$ (for $i + j$ odd) in the dimer model on $\mathcal{A}_{0,1,k}$ when k is even. Therefore the generating function for the averages $\langle 1 - D_{i,j} \rangle_{0,0,2k-1}$ on the even faces (with $i + j = 0 \bmod 2$) of the dimer model on $A_{0,0,2k-1}$ reads:

$$\sum_{\substack{i,j \in \mathbb{Z} \\ i+j \text{ even}}} \langle 1 - D_{i,j} \rangle_{0,0,2k-1} \, x^i \, y^j = \rho^{(0,0)}(x^{-1}, y^{-1}, z)|_{z^{2k-1}} = \rho^{(0,0)}(x,y,z)|_{z^{2k-1}}$$

by use of the obvious symmetries $x \leftrightarrow x^{-1}$ and $y \leftrightarrow y^{-1}$ of $\rho^{(0,0)}$ (2.12), and where the notation $f|z^m$ stands for the coefficient of z^m in the power expansion of f as a series of z. Similarly, the generating function for the averages $\langle 1 - D_{i,j} \rangle_{0,1,2k}$ on the even faces of the dimer model on $A_{0,1,2k}$ reads:

$$\sum_{\substack{i,j \in \mathbb{Z} \\ i+j \text{ even}}} \langle 1 - D_{i,j} \rangle_{0,1,2k} \, x^i \, y^j = y\, \rho^{(0,0)}(x^{-1}, y^{-1}, z)|_{z^{2k-1}} = y\, \rho^{(0,0)}(x,y,z)|_{z^{2k}}$$

We have similar expressions for the averages on odd faces, involving $\rho^{(0,1)}$.

The singularities of these two expressions are determined by the denominator of $\rho^{(0,0)}(x,y,z)$ given by (2.12).
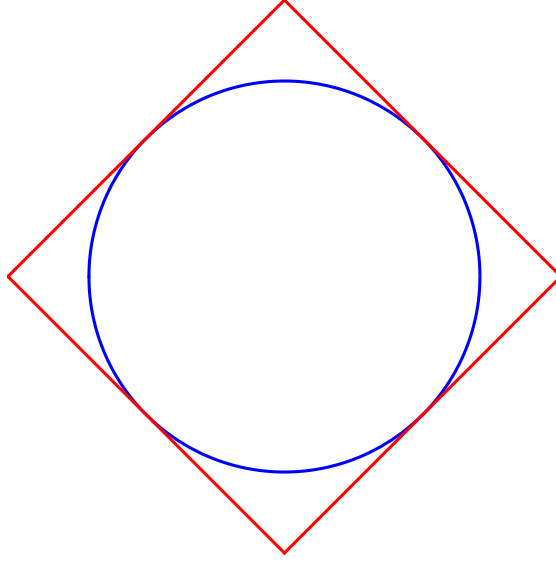
FIGURE 2. Arctic circle for the trivial initial data. The corners are frozen and the center is disordered.

Following the general theory of singularities of multivariate series [33, 34, 35], to explore the behavior of the coefficients $\rho_{i,j,k}^{(0,0)}$ for large i, j, k and $\frac{i}{k} = u$, $\frac{j}{k} = v$ finite, we must blow up the singular point $x = y = z = 1$ by taking $x \to 1-tx$, $y \to 1-ty$ and $z \to 1+t(ux+vy)$ and then expand the denominator in powers of t. Up to order t^2 we have:

$$z^{-1} + z - \frac{1}{2}(x^{-1} + x + y^{-1} + y) = \frac{t^2}{2}((2u^2 - 1)x^2 + (2v^2 - 1)y^2 + 4uvxy) + O(t^3)$$

Let us define $H(x,y) = (2u^2 - 1)x^2 + (2v^2 - 1)y^2 + 4uvxy$. We now look for a polynomial in u, v. Imposing $H(x,y) = 0$ and $\frac{\partial}{\partial x}H(x,y) = 0$ we can eliminate x and y. The polynomial in u, v is given by:

(2.13)
$$P(u,v) = 2(u^2 + v^2) - 1$$

The zero locus of P defines the arctic circle (see Fig. 2). This is the circle inscribed into the square domain $|u| + |v| = 1$, which corresponds to the limiting domain of non-zero values of $\rho_{i,j,k}$ for $k \to \infty$ while $\frac{i}{k} = u$, $\frac{j}{k} = v$.

3. TOROIDAL INITIAL DATA I: THE 2×2 CASE

In this section we will focus on a very specific initial data, which has period two in both i and j directions, namely:

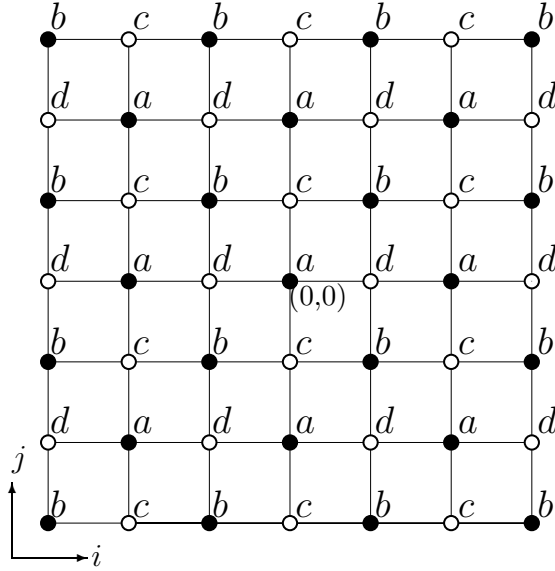$$t_{i+2,j} = t_{i,j} \qquad t_{i,j+2} = t_{i,j}$$

FIGURE 3. Initial data with period 2 in directions i, j. The white and black points corresponds to the planes $k = 0$ and $k = 1$ respectively.

More precisely, we set (see Fig. 3):

$$(3.1) \qquad t_{i,j} = \begin{cases} a & \text{if } i = 0, j = 0 \bmod 2 \\ b & \text{if } i = 1, j = 1 \bmod 2 \\ c & \text{if } i = 0, j = 1 \bmod 2 \\ d & \text{if } i = 1, j = 0 \bmod 2 \end{cases}$$

Remarkably, this particular initial data allows us to still find an exact and simple solution for the T-system. At the same time it provides us with an illustrative example on how to compute the arctic curves for non-uniform initial data. We will see that the ratios $L_{i,j,k}$ and $R_{i,j,k}$ appearing in (2.4) have a certain periodicity that allows to reduce the problem to a finite linear system of 4 equations (each for different values of the ratios).

3.1. **Exact solution of the T-system with 2×2 periodic initial data.** The corresponding T-system actually coincides with the so-called Q-system for $\widehat{A}_1$. The exact solution to this T-system with doubly periodic initial data is given by:

Lemma 3.1.

$$(3.2) \qquad T_{i,j,k} = \left(\frac{a^2 + b^2}{cd}\right)^{\lfloor \frac{k}{2} \rfloor \lfloor \frac{k+1}{2} \rfloor} \left(\frac{c^2 + d^2}{ab}\right)^{\lfloor \frac{k-1}{2} \rfloor \lfloor \frac{k}{2} \rfloor} \begin{cases} t_{i,j} & , \text{ if } k = 0, 1, \bmod 4 \\ t_{i+1,j+1} & , \text{ if } k = 2, 3, \bmod 4 \end{cases}$$

for $t_{i,j}$ as in (3.1).

Proof. By induction on k. $\qquad\qquad\qquad\qquad\qquad\qquad\qquad\qquad\qquad\qquad\qquad\quad$ $\square$

3.2. **Density: exact derivation.** As explained before, we may consider various density functions $\rho_{i,j,k}^{(\epsilon,\eta)}$ that measure the average $\langle 1 - D_{\epsilon,\eta}\rangle_{i,j,k}$ on the face (ϵ,η) of the dimer model on $\mathcal{A}_{i,j,k}$. For odd k this is equal to the average $\langle 1 - D_{\epsilon-i,\eta-j}\rangle_{0,0,k}$ of the dimer model on $\mathcal{A}_{0,0,k}$ (in which the central face is of a type).

Let us consider only even faces of type a or b, namely $\epsilon = \eta = 0$ or 1, and k odd. Then the density $\rho^{(0,0)}(x^{-1}, y^{-1}, z)|_{x^{\mathrm{even}}y^{\mathrm{even}}}$ generates $\langle 1 - D_{i,j}\rangle_{0,0,k}$ on a-type faces with both i, j even, while $xy\left(\rho^{(1,1)}(x^{-1}, y^{-1}, z)|_{x^{\mathrm{even}}y^{\mathrm{even}}}\right)$ generates $\langle 1 - D_{i,j}\rangle_{0,0,k}$ on b-type faces with both i, j odd. By considering odd powers of x, y instead, we have also access to averages of $1 - D_{i,j}$ for $\mathcal{A}_{1,1,k}$ (in which the central face is of b type).

Now that we have a solution for the T-system, we can directly compute the ratios in the recurrence relation for the density (2.4). We note that the ratio $L_{i,j,k}$ is periodic (as well as $R_{i,j,k}$, from the relation $L_{i,j,k} + R_{i,j,k} = 1$). We have indeed an obvious periodicity on the constant k planes. Defining $e_1 = (2,0,0)$ and $e_2 = (0,2,0)$, we have that $L_{(i,j,k)} = L_{(i,j,k)+me_1+ne_2}$ where $m, n \in \mathbb{Z}$ (the same for $R_{i,j,k}$). However, by using the exact solution (3.2), we find another less obvious periodicity in the direction $e_3 = (1,1,2)$ as well. This is summarized in the following:

Lemma 3.2. *The coefficients $L_{i,j,k}, R_{i,j,k}$ corresponding to the 2×2 periodic solution (3.2) of the T-system have the following periodicity:*

$$L_{(i,j,k)} = L_{(i,j,k)+me_1+ne_2+pe_3} \qquad (m, n \in \mathbb{Z}, p \geq 0).$$

and similarly for $R_{i,j,k} = 1 - L_{i,j,k}$.

Proof. By inspection. $\qquad\square$

Let us first derive $\rho^{(0,0)}(x, y, z)$. Define the following partial generating functions:

$$(3.3) \qquad \rho^{(i_0,j_0,k_0)}(x, y, z) = \sum_{m,n\in\mathbb{Z},p\geq 0} \rho_{(i_0,j_0,k_0)+me_1+ne_2+pe_3}^{(0,0)} x^{i_0+2m+p}y^{j_0+2n+p}z^{k_0+2p}$$

where (i_0, j_0, k_0) are in the unit cell for the periodicities of Lemma 3.2, namely $(i_0, j_0, k_0) \in P = \{(0,0,1), (1,1,1), (1,0,0), (0,1,0)\}$. In terms of these the full density generating function is simply

$$\rho^{(0,0)}(x, y, z) = \sum_{(i_0,j_0,k_0)\in P} \rho^{(i_0,j_0,k_0)}(x, y, z)$$

Using the recurrence relation for the density (2.4) and the initial conditions $\rho_{i,j,1}^{(0,0)} = \delta_{i,0}\delta_{j,0}$, $\rho_{i,j,0}^{(0,0)} = 0$, we end up with the following linear system:

$$(3.4) \quad \begin{pmatrix} \frac{1}{z} & \frac{(x^2+1)(\tau-1)}{x} & -\frac{(y^2+1)\tau}{y} & z \\ z & \frac{(y^2+1)(\tau-1)}{y} & -\frac{(x^2+1)\tau}{x} & \frac{1}{z} \\ -\frac{(y^2+1)\sigma}{y} & \frac{1}{z} & z & \frac{(x^2+1)(\sigma-1)}{x} \\ -\frac{(x^2+1)\sigma}{x} & z & \frac{1}{z} & \frac{(y^2+1)(\sigma-1)}{y} \end{pmatrix} \begin{pmatrix} \rho^{(0,0,1)}(x,y,z) \\ \rho^{(0,1,0)}(x,y,z) \\ \rho^{(1,0,0)}(x,y,z) \\ \rho^{(1,1,1)}(x,y,z) \end{pmatrix} = \begin{pmatrix} 1 \\ 0 \\ 0 \\ 0 \end{pmatrix}$$

where we have used the parametrizations of weights:

$$a = b\sqrt{\frac{\sigma}{1-\sigma}} \qquad \text{and} \qquad c = d\sqrt{\frac{\tau}{1-\tau}}$$

It is worth noticing that even though we started with 4 arbitrary values a, b, c, d in our initial data in the 2×2 torus, the corresponding system for the density only depends on 2 parameters, the ratios a/b and c/d. As we saw in the case of the uniform initial data, the arctic curve is determined by the zero locus of the denomiator of the density functions. Here, this denominator is given by the determinant of the above system of 4 equations. Defining

$$(3.5) \qquad \alpha = 16\sigma(1-\sigma)\tau(1-\tau) = \frac{16}{\left(\frac{a}{b} + \frac{b}{a}\right)^2 \left(\frac{c}{d} + \frac{d}{c}\right)^2}$$

then, up to a factor of xyz, the determinant reads:

$$(3.6) \quad D(x,y,z) = \frac{\alpha}{16}(x^2 - y^2)^2(x^2y^2 - 1)^2 z^4 - x^2y^2\left(xy - z^2\right)\left(y - xz^2\right)\left(x - yz^2\right)\left(1 - xyz^2\right)$$

The actual density $\rho^{(0,0)}(x,y,z)$ however depends explicitly on σ, τ, not just on α. It has the form $\rho^{(0,0)}(x,y,z) = \frac{Q^{(0,0)}(x,y,z)}{D(x,y,z)}$, with D as in (3.6), and $Q^{(0,0)}$ the following polynomial of x, y, z:

$$\begin{aligned}
Q^{(0,0)}(x,y,z) = {} & xyz\left\{(-x^2y^2(1-z^2)(z(x(1-xyz^2) + y(xy - z^2)) + xy(1-z^4))\right. \\
& -xy(x-y)(1-xy)z^2(x(1-xyz^2) + y(xy-z^2))\sigma + x^2y^2(x-y)(1-xy)z(1-z^4)\tau \\
(3.7) \quad & +xy(x^2-y^2)(1-x^2y^2)z^2(1-z^2)\sigma\tau - (x-y)(x^2-y^2)(1-xy)(1-x^2y^2)z^3\sigma\tau(1-\tau)\right\}
\end{aligned}$$

Similarly, the density $\rho^{(1,1)}(x,y,z)$ solves the same system (3.4), but with the r.h.s. replaced by $(0, xy, 0, 0)^t$, due to the initial conditions $\rho_{i,j,1}^{(1,1)} = \delta_{i,1}\delta_{j,1}$ and $\rho_{i,j,0}^{(1,1)} = 0$. Alternatively, $\rho^{(1,1)}/(xy)$ is obtained by interchanging $a \leftrightarrow b$ and $c \leftrightarrow d$ in the expression for $\rho^{(0,0)}$, namely by performing the substitutions $\sigma \to 1 - \sigma$ and $\tau \to 1 - \tau$. These produce a new numerator $Q^{(1,1)}$, but leave the denominator $D(x,y,z)$ unchanged.

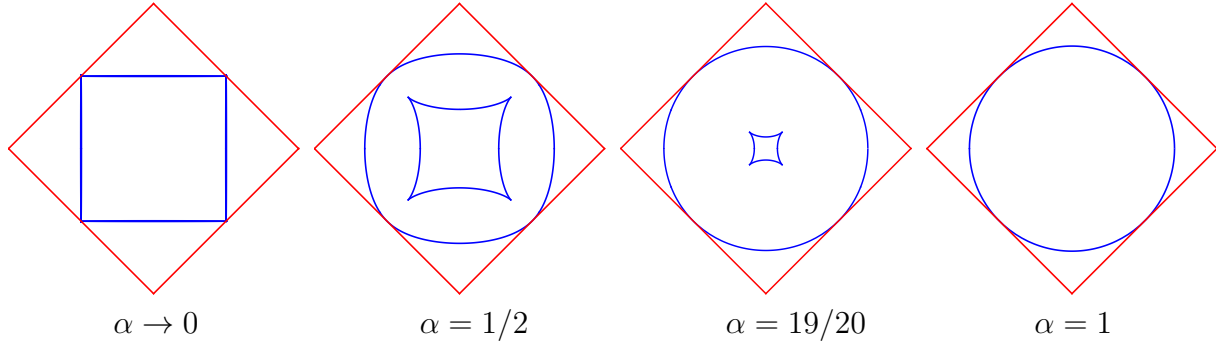| $\alpha \to 0$ | $\alpha = 1/2$ | $\alpha = 19/20$ | $\alpha = 1$ |

FIGURE 4. Arctic curves for the periodic initial data corresponding to different values of α.

3.3. **Arctic curve.** Using the same procedure as for the uniform initial data, we look at the zero locus $D(x, y, z) = 0$. We take $x \to 1 - tx$, $y \to 1 - ty$ and $z \to 1 + t(ux + vy)$ and then expand $D(1 - tx, 1 - ty, 1 + t(ux + vy)) = t^4 H(x, y) + O(t^5)$ at leading order in t (which in this case turns out to be t^4). As above imposing $H(x, y) = 0$ and $\frac{\partial}{\partial x} H(x, y) = 0$ we can eliminate x and y. We finally get the following polynomial $P_\alpha(u, v)$:

$$
\begin{aligned}
P_\alpha(u, v) =&(1 - \alpha)^3 + 16\alpha^2(u^8 + v^8) + 8(4 - 5\alpha)\alpha(u^6 + v^6) + 32\left(\alpha^2 + 2(2 - \alpha)^2\right) u^4 v^4 \\
&+ \left((4 - \alpha)^2 - 24\alpha\right)(1 - \alpha)\left(u^4 + v^4\right) + 8\left(6\alpha^2 - (4 - \alpha)^2\right) u^2 v^2\left(u^2 + v^2\right) \\
&+ 2\left(48 - (4 - \alpha)^2\right)(1 - \alpha)u^2 v^2 - 2(1 - \alpha)^2(4 - \alpha)(u^2 + v^2) + 64(2 - \alpha)\alpha u^2 v^2(u^4 + v^4)
\end{aligned}
$$

(3.8)

Notice that this polynomial depends only on the single parameter α of (3.5). The singularity curve corresponds to the zero locus of $P(u, v)$ for a given α. Let us examine a few limiting cases of interest.

For $\alpha = 1$, the curve degenerates into:

$$P_1(u, v) = 8(u^2 + v^2)^3(2u^2 + 2v^2 - 1)$$

and we recover the same result as in the uniform case ($\sigma = \tau = 1/2$), namely the arctic circle $2u^2 + 2v^2 = 1$ of Fig.2.

For $\alpha = 0$, the curve degenerates into:

$$P_0(u, v) = (4u^2 - 1)^2(4v^2 - 1)^2$$

namely into the square with edges $u = \pm\frac{1}{2}$, $|v| \leq \frac{1}{2}$ and $v = \pm\frac{1}{2}$, $|u| \leq \frac{1}{2}$, inscribed into the domain $|u| + |v| = 1$.

We have represented two more somewhat generic cases, with $\alpha = \frac{1}{2}$ and $\alpha = 1 - \frac{1}{20}$ in Fig. 4. In addition to the actual external arctic curve tangent to the square $|u| + |v| = 1$ at the 4 points $(u, v) = (\pm\frac{1}{2}, \pm\frac{1}{2})$, we note the existence of an internal curve with 4 cusps at positions $(u, v) = (\pm\frac{\sqrt{1-\alpha}}{2}, \pm\frac{\sqrt{1-\alpha}}{2})$ along the $u = \pm v$ lines. In addition to the frozen and temperate regions, we obtain a new "bubble" inside, often called the *facet* domain.
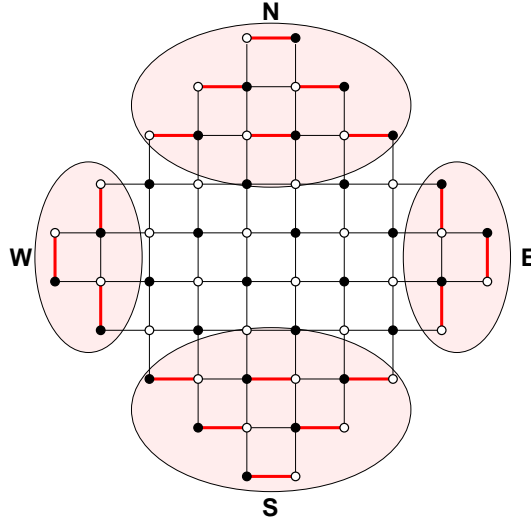
FIGURE 5. The four frozen dimer configurations pertaining to the four (N,S,E,W) corners of the Aztec diamond graph.

The facet domain disappears exactly at $\alpha = 1$, in which case we are left with simply the arctic circle, whereas it is "maximal" at $\alpha = 0$, where it becomes an inscribed square, and gets identified with the external arctic curve, so that the temperate region is squeezed and disappears. The parameter α clearly governs the size of this facet domain.

The phase structure with a central facet shown in Fig.4 is similar to that found for the "square-octagon fortress" case, where the corresponding arctic curve is of *same* degree 8 as ours (3.8) (see Figure 18 of [26]).

3.4. **Physical interpretation and phase diagram.**

3.4.1. *Uniform case.* We have seen that the density $\rho_{i,j,k}$ (2.3) is a measure of the expectation value, within the statistical ensemble of dimer configurations of the Aztec domain of size k, of the observable $1 - D_{i,j}$, where $D_{i,j}$ is the number of dimers occupying the edges around a given face (i, j) of the domain with fixed parity of $i + j$. It therefore measures the imbalance between the empty squares configurations ($D_{i,j} = 0$) and the maximally occupied ones ($D_{i,j} = 2$).

The asymptotics of the coefficients $\rho_{i,j,k}^{(0,0)}$ for large i, j, k with $i/k = u$ and $j/k = v$ of the density generating series $\rho^{(0,0)}(x, y, z)$ (2.12) for the trivial initial data can be extracted by using for instance general theorems of Baryshnikov and Pemantle [2] (Theorem 3.7). The result reads:

$$(3.9) \qquad \rho_{i,j,k}^{(0,0)} =\sim \frac{2}{\pi k} \frac{\delta_{i+j+k,1}^{[2]}}{\sqrt{1 - 2(u^2 + v^2)}}$$
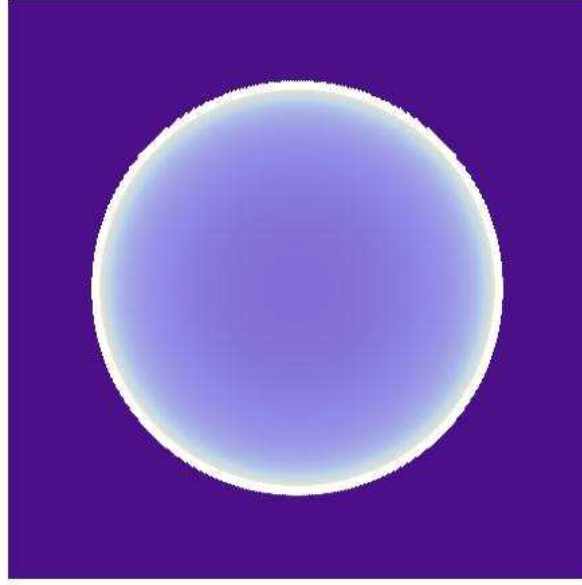
FIGURE 6. Density profile for the coefficients $\rho_{i,j,k}^{(0,0)}$ given in (3.9) for $k = 211$ and $-k \leq i, j \leq k$.

This scaling function $\rho_{i,j,k} \sim u(i,j,k)$ appeared in [6] (see p.26, where it is found to obey the differential equation $\frac{\partial^2}{\partial z^2} u = \frac{1}{2}\left(\frac{\partial^2}{\partial x^2} + \frac{\partial^2}{\partial y^2} \right) u$).

We display in Fig. 6 the density profile for this asymptotic value of $\rho_{i,j,k}^{(0,0)}$.

The standard explanation for the arctic circle in the uniform initial data case is that the dimer configurations that contribute to the partition function $T_{i,j,k}$ tend to be in a fundamental crystalline state in the vicinity of the corners of the square domain $|i| + |j| \leq |k|$. There are four distinct such states, each corresponding to a (N,S,E,W) corner, characterized by an occupation number $D_{i,j} = 1$ on each face (i,j) (see Fig.5). Away from the corners, the dimer model has a non-trivial entropy, and the competition between order and disorder gives rise to a separating critical curve in the continuum thermodynamic limit when $k \to \infty$ with $\frac{i}{k} = u$ and $\frac{j}{k} = v$ fixed, between a frozen phase (next to the corners) and a so-called temperate phase (in the center). Outside of the critical curve, the density decays exponentially as $k \to \infty$ to 0, as each square tends to be occupied by a single dimer, while inside the curve it decreases as a power law $\propto \frac{1}{k}$, whereas the coefficient tends to the non-zero function $2/(\pi \sqrt{1 - 2(u^2 + v^2)})$, singular on the arctic curve. This function indicates a growing local disorder in the dimer configurations, maximum at the center of the Aztec domain. We have represented the values of the rescaled density function $k|\rho_{i,j,k}^{(0,0)}|$ for fixed $k = 85$, $-k \leq i, j \leq k$ and $i + j + k = 1 \mod 2$.
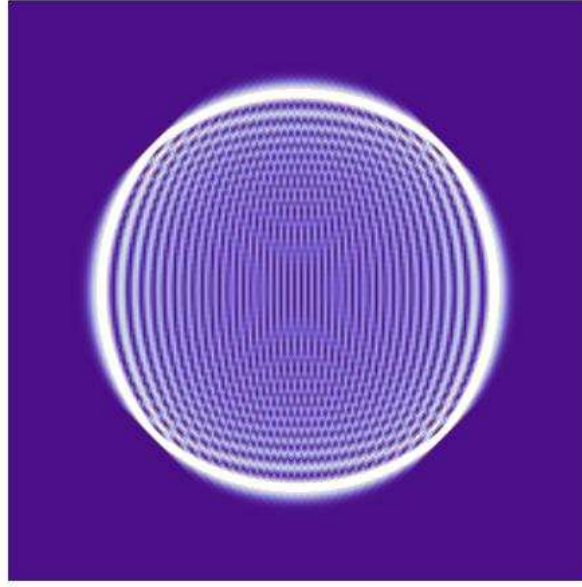
FIGURE 7. Density profile for the trivial initial data. The dark color corresponds to $\rho_{i,j,k} = 0$ and brighter color to larger $\rho_{i,j,k}$. The scale of colors is arbitrary.
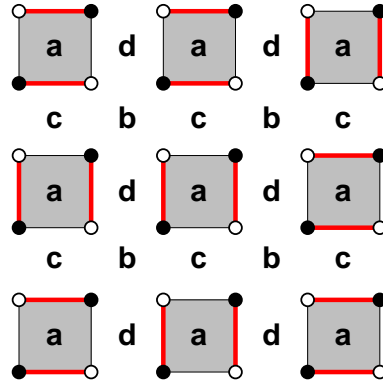

FIGURE 8. The typical dominant dimer configurations for odd k when $a \to 0$: each a-type face is occupied by two dimers, with two arbitrary choices of orientation on each a-type face.

3.4.2. 2×2 *periodic case.* To understand the emergence of a new (facet) central phase, let us first consider the simple case $\sigma = 0$. We saw that in that case, the arctic curve degenerates to an inscribed square and the temperate region disappears. This is attained for instance by fixing $b, c, d > 0$ and letting $a \to 0$ in the various density functions.
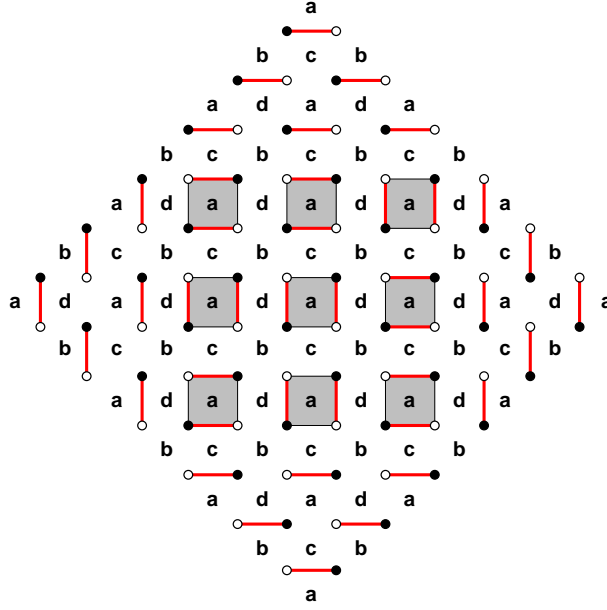
FIGURE 9. The typical dominant dimer configurations for $k = 7$ when $a \to 0$: each a-type face in the inscribed square region is occupied by two dimers, with two arbitrary choices of orientation on each a-type face (shaded).

It is clear that if a is very small, the Boltzmann weight of maximally occupied dimer configurations around the a faces becomes the dominant contribution to the partition function (see Fig.8 for an illustration). We expect therefore a phase where the a type faces are occupied by two dimers, with arbitrary (vertical or horizontal) orientation. This phase is globally crystalline, from the pinning of the dimers to the a-type faces that form a square sublattice, but retains some non-trivial entropy, from the arbitrary orientation of the pair of dimers at each site, hence the name facet. Note that this also imposes another square sublattice of empty faces. The corresponding value of $\langle 1-D \rangle$ for k odd is -1 on the former sublattice, and 1 on the latter.

More precisely, for $\sigma = 0$ the solution of the system (3.4) and its companion for $\epsilon = \eta = 1$ above lead to:

$$
\begin{aligned}
\rho^{(0,0)}(x,y,z) \;=\; & \frac{z}{(xy - z^2)(x - yz^2)(y - xz^2)(1 - xyz^2)} \times \\
& \{ x^2 y^2 - xyz^2 - x^3 yz^2 - x^2 y^2 z^2 - xy^3 z^2 - x^3 y^3 z^2 - x^2 yz^3 - xy^2 z^3 - x^3 y^2 z^3 \\
& - x^2 y^3 z^3 + x^2 z^4 + x^2 y^2 z^4 + x^2 y^4 z^4 + x^2 yz^5 + xy^2 z^5 + x^3 y^2 z^5 + x^2 y^3 z^5 + x^2 y^2 z^6 \} \\
& + \tau \frac{z^3 (x^2 - y^2)(1 - x^2 y^2)}{(xy - z^2)(x - yz^2)(y - xz^2)(1 - xyz^2)}
\end{aligned}
$$

and:

$$\frac{\rho^{(1,1)}(x,y,z)}{xy} = \frac{z}{(xy-z^2)(x-yz^2)(y-xz^2)(1-xyz^2)} \times$$
$$\{x^2y^2 + x^2yz + xy^2z + x^3y^2z + x^2y^3z + y^2z^2 + x^2y^2z^2 + x^4y^2z^2 - x^2yz^3$$
$$-xy^2z^3 - x^3y^2z^3 - x^2y^3z^3 - xyz^4 - x^3yz^4 - x^2y^2z^4 - xy^3z^4 - x^3y^3z^4 + x^2y^2z^6\}$$
$$-\tau\frac{z^3(x^2-y^2)(1-x^2y^2)}{(xy-z^2)(x-yz^2)(y-xz^2)(1-xyz^2)}$$

with $\tau = \frac{c^2}{c^2+d^2}$. As explained above, the final generating function for $\langle 1 - D_{i,j}\rangle_{0,0,2k-1}$ for $i+j$ even is obtained by extracting the even powers of x, y from $\rho^{(0,0)}$ and the odd powers of x, y from $\rho^{(1,1)}/(xy)$, namely by forming:

$$U(x,y,z) = \frac{1}{4}(A(x,y,z) + A(-x,y,z) + A(x,-y,z) + A(-x,-y,z))$$
$$+\frac{1}{4}(B(x,y,z) - B(-x,y,z) - B(x,-y,z) + B(-x,-y,z))$$

where $A = \rho^{(0,0)}$, and $B = \rho^{(1,1)}/(xy)$ above. Similarly, the generating function for $\langle 1 - D_{i,j}\rangle_{1,1,2k}$ for $i+j$ even is obtained by extracting the odd powers of x, y from $\rho^{(0,0)}$ and the even powers of x, y from $\rho^{(1,1)}/(xy)$, namely by forming:

$$V(x,y,z) = \frac{1}{4}(A(x,y,z) - A(-x,y,z) - A(x,-y,z) + A(-x,-y,z))$$
$$+\frac{1}{4}(B(x,y,z) + B(-x,y,z) + B(x,-y,z) + B(-x,-y,z))$$

Let us denote by $f_k(x,y)$ the coefficient of z^k in the series expansion of $f(x,y,z)$, and by $[n]_x = \frac{x^n - x^{-n}}{x - x^{-1}}$ and similarly for y. Noting the generating functions

$$\sum_{n\geq 0}[n]_x[n]_y z^n = \frac{x^2y^2z(1-z^2)}{(xy-z^2)(x-yz^2)(y-xz^2)(1-xyz^2)}$$

$$\sum_{n\geq 1}[n+1]_x[n-1]_y z^n = \frac{yz^2(y + x^2y + x^4y - xz - x^3z - xy^2z - x^3y^2z + x^2yz^2)}{(xy-z^2)(x-yz^2)(y-xz^2)(1-xyz^2)}$$

and expressing $U(x,y,z)$ and $V(x,y,z)$ in terms of these, we finally get:

$$U_{4k-1}(x,y) = [2k]_x[2k]_y - [2k-1]_x[2k-1]_y$$
$$U_{4k-3}(x,y) = \tau([2k-2]_x[2k]_y - [2k-3]_x[2k-1]_y)$$
$$+(1-\tau)([2k]_x[2k-2]_y - [2k-1]_x[2k-3]_y)$$
$$V_{4k-1}(x,y) = \tau([2k-1]_x[2k+1]_y - [2k-2]_x[2k]_y)$$
$$+(1-\tau)([2k+1]_x[2k-1]_y - [2k]_x[2k-2]_y)$$
$$V_{4k-3}(x,y) = [2k-1]_x[2k-1]_y - [2k-2]_x[2k-2]_y$$

$$\alpha = 1 \qquad\qquad \alpha = 0.98 \qquad\qquad \alpha = 0.5 \qquad\qquad \alpha = 0.01$$
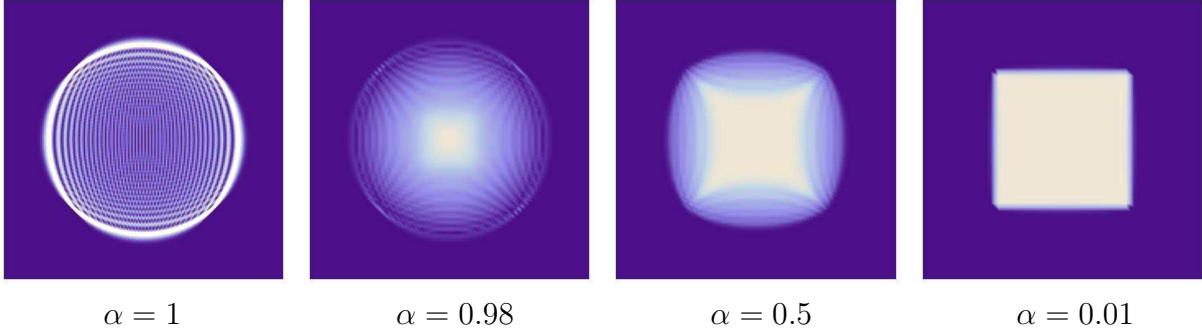
FIGURE 10. Density profiles for $\rho_{i,j,k}$ for the periodic initial data corresponding to different values of α. We fixed $b = c = d = 1$ and vary a accordingly to get the α shown in the profiles (see (3.5))

Recall that the U's correspond to the averages in the dimer model on Aztec graphs with a central face of a type, while the V's correspond to the averages in the dimer model on Aztec graphs with a central face of b type. The case U_{4k-1}, V_{4k-3} display an alternance of ± 1 on (even, even)/(odd,odd) faces. This is in agreement with the typical dominant configuration represented in Fig.9, corresponding to $U_7(x,y)$: the facet occupies exactly the inscribed square $|i|, |j| \leq 3$, while outside this domain each face is occupied by a single dimer, i.e. we have four corners frozen in their respective fundamental states with zero entropy. The cases U_{4k-3}, V_{4k-1} also have a central facet square region with the same alternance of ± 1, but have a thin boundary region around the square where the averages explicitly depend on τ.

We conclude that asymptotically the density is identically zero outside of the inscribed square $|u|, |v| \leq \frac{1}{2}$, while inside it takes finite nonzero values that alternate on two square sublattices. The arctic curve is nothing but the exact phase separation, here reduced to the inscribed square $|u| = \frac{1}{2}, |v| \leq \frac{1}{2}$ and $|v| = \frac{1}{2}, |u| \leq \frac{1}{2}$.

More generally, when $1 > \sigma, \tau > 0$, we still expect frozen corner phases and a central facet phase induced by the pinning on one sublattice of configurations of pairs of parallel dimers, corresponding to the smallest weights among a, b and c, d. The plot of the arctic curve (3.8) shows that a disordered phase separates the facet from the frozen corners. In both the frozen corners and the facet, the convergence of $\rho_{i,j,k}$ for $i/k = u, j/k = v$ fixed is exponential in k. As explained above, the behavior of $\rho^{(0,0)}$ in the disordered phase is connected to the singularity $x = y = z = 1$ of both numerator (3.7) and denominator (3.6). We find that the leading orders in the t expansion for $x \to 1 - tx, y \to 1 - ty, z \to 1 - tz$ are respectively $Q^{(0,0)} \sim t$ if $\sigma \neq \frac{1}{2}$, and $Q^{(0,0)} \sim t^2$ otherwise, while $D \sim t^4$ in all cases. We deduce that if $\sigma = \frac{1}{2}$ then $\rho_{i,j,k}$ for $i/k = u, j/k = v$ fixed tends to 0 algebraically, as k^{-1}, and diverges at the boundary of the temperate zone (both along the facet border and the frozen corners border). However if $\sigma \neq \frac{1}{2}$, we find that $\rho_{i,j,k}$ tends to a scaling function

without any global rescaling. We display in Fig.10 a picture of the values of $|\rho_{i,j,k}^{(0,0)}|$ for size $k = 85$, $-k \leq i,j \leq k$ and both i and j even.

4. TOROIDAL INITIAL DATA II: THE m-TOROIDAL CASE

In this section, we introduce the T-system with initial data wrapped on a torus involving $4m$ arbitrary initial values. This particular choice is exactly solvable, and leads to the exact derivation of higher degree arctic curves.

4.1. **Exact solution of the T-system with m-toroidal initial data.**

Definition 4.1. *Let us consider the following condition on the initial data* $\{t_{i,j}\}_{i,j\in\mathbb{Z}}$ *of the* T-*system* (2.1):

$$(4.1) \qquad t_{i+m,j-m} = t_{i,j} \qquad \text{and} \qquad t_{i+2,j+2} = t_{i,j} \qquad (i,j \in \mathbb{Z})$$

Initial data with this property will be called m-*toroidal boundary conditions. The corresponding torus of the* $\mathbb{Z}^2$ *plane is generated by the two vectors* $\vec{e}_1 = (m,-m,0)$ *and* $\vec{e}_2 = (2,2,0)$.

It is easy to show that any solution of the T-system with m-toroidal boundary conditions satisfies the same toroidal conditions, namely that: $T_{i+m,j-m,k} = T_{i,j,k}$ and $T_{i+2,j+2,k} = T_{i,j,k}$ for all $i,j \in \mathbb{Z}$ and $k \in \mathbb{Z}_+$, and $i + j + k = 1$ mod 2.

Quite remarkably, there is an explicit expression for the solution of the T-system for m-toroidal boundary conditions.

Let us first denote respectively by a_i, b_i, c_i, d_i the initial data corresponding to a fundamental domain in the planes $k = 0$ and $k = 1$, namely (see Fig.11 for an illustration):

$$(4.2) \qquad \begin{aligned} a_i &= T_{i+1,-i,0} = t_{i+1,-i} & b_i &= T_{i+2,-i+1,0} = t_{i+2,-i+1} \\ c_i &= T_{i,-i,1} = t_{i,-i} & d_i &= T_{i+1,-i+1,1} = t_{i+1,-i+1} \end{aligned}$$

for $i \in \mathbb{Z}$. The sequences a_i, b_i, c_i, d_i $i \in \mathbb{Z}$ are clearly periodic with period m, as a direct consequence of the conditions (4.1). Let us further introduce two m-periodic sequences x_i, y_i defined as:

$$(4.3) \qquad x_i = \frac{c_i d_{i+1} + c_{i+1} d_i}{a_i b_i} \qquad \text{and} \qquad y_i = \frac{a_{i-1} b_i + a_i b_{i-1}}{c_i d_i} \qquad (i \in \mathbb{Z})$$

Note that we have:

$$T_{i+1,-i,2} = x_i b_i \qquad T_{i+2,-i+1,2} = x_i a_i$$

We also define for $n \geq 1$ and $i \in \mathbb{Z}$ the quantities:

$$(4.4) \qquad u_{n,i} = \prod_{\ell=0}^{n-1} (x_{i-\ell-1})^{\frac{n+1}{2} - \left|\frac{n-1}{2} - \ell\right|} \qquad v_{n,i} = \prod_{\ell=0}^{n-1} (y_{i-\ell-1})^{\frac{n+1}{2} - \left|\frac{n-1}{2} - \ell\right|}$$
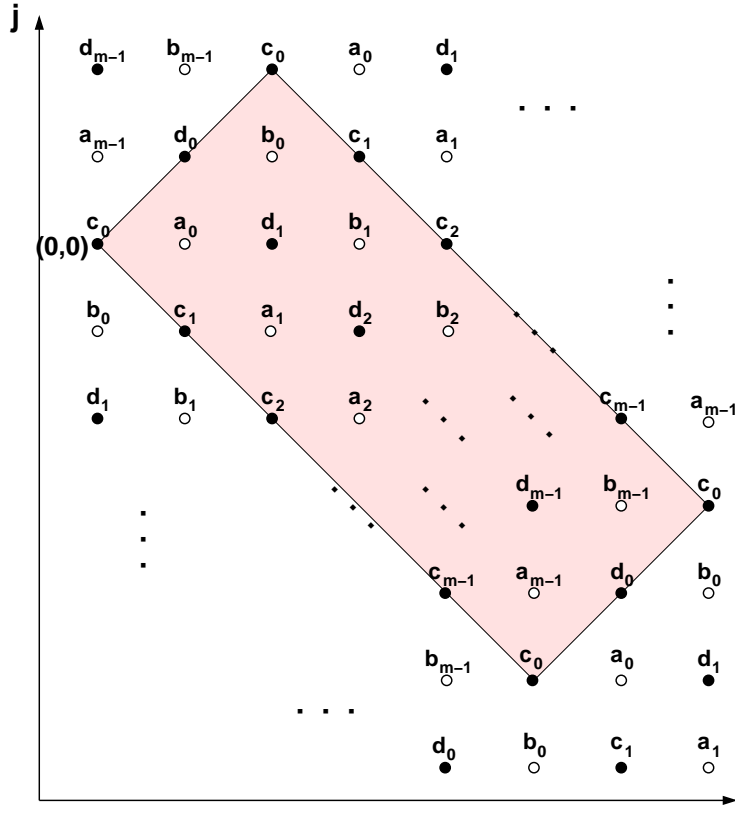
FIGURE 11. The initial data of the m-toroidal T-system in the (i, j) plane. The empty circles correspond to $k = 0$ and the filled circles to $k = 1$. We have shaded a fundamental domain for the corresponding torus.

with the convention that $u_{0,i} = u_{-1,i} = u_{-2,i} = 1$ and similarly for v. Finally, let $\theta_{i,j,k}$ be defined for $i, j \in \mathbb{Z}$ and $k \in \mathbb{Z}_+$ as:

$$\theta_{i,j,k} = T_{i+\lfloor \frac{k}{2} \rfloor, j+\lfloor \frac{k}{2} \rfloor, k \bmod 2} \tag{4.5}$$

In particular, for $k = 0, 1$ we have from the initial data (2.2):

$$\theta_{i,j,i+j+1 \bmod 2} = t_{i,j}. \tag{4.6}$$

With the above definitions, the following theorem gives the exact value of the solution $T_{i,j,k}$ of the T-system with m-toridal boundary conditions.

Theorem 4.2. *With the above definitions for $u_{n,i}, v_{n,i}, \theta_{i,j,k}$, the solution $T_{i,j,k}$ to the T-system with m-toroidal boundary conditions (4.1) given by (4.2) reads explicitly:*

$$T_{i,j,k} = u_{k-1, \frac{i-j+k-1}{2}} \, v_{k-2, \frac{i-j+k-1}{2}} \, \theta_{i,j,k} \tag{4.7}$$

Moreover, we have the following explicit values for the cross-ratios $L_{i,j,k}$ and $R_{i,j,k}$, with the notations $\alpha = \frac{i-j}{2}$, $\beta = \frac{i-j-1}{2}$, and $\delta_{i,j}^{[p]} = \delta_{i-j,0 \bmod p}$:

$$
L_{i,j,k} = \frac{T_{i+1,j,k}T_{i-1,j,k}}{T_{i,j,k+1}T_{i,j,k-1}} = \delta_{i+j+k,0}^{[4]} \left(\delta_{k,0}^{[2]} \frac{a_\alpha b_{\alpha-1}}{a_\alpha b_{\alpha-1} + a_{\alpha-1} b_\alpha} + \delta_{k,1}^{[2]} \frac{c_{\beta+1} d_\beta}{c_\beta d_{\beta+1} + c_{\beta+1} d_\beta} \right)
$$

$$
+ \delta_{i+j+k,2}^{[4]} \left(\delta_{k,0}^{[2]} \frac{a_{\alpha-1} b_\alpha}{a_\alpha b_{\alpha-1} + a_{\alpha-1} b_\alpha} + \delta_{k,1}^{[2]} \frac{c_\beta d_{\beta+1}}{c_\beta d_{\beta+1} + c_{\beta+1} d_\beta} \right)
$$

$$
R_{i,j,k} = \frac{T_{i,j+1,k}T_{i,j-1,k}}{T_{i,j,k+1}T_{i,j,k-1}} = 1 - L_{i,j,k}
$$

Proof. For $T_{i,j,k}$ as in the statement of the theorem, let us compute the ratios $L_{i,j,k}$ and $R_{i,j,k}$. To this end, we note that by definition:

$$
(4.8) \qquad \frac{u_{k,a}}{u_{k-1,a}} = \prod_{\ell=0}^{\lfloor \frac{k-1}{2} \rfloor} x_{a-k+\ell} \quad \text{and} \quad \frac{u_{k-1,a-1} \, u_{k-1,a}}{u_{k-2,a-1} \, u_{k,a}} = \begin{cases} 1 & \text{if } k \text{ even} \\ 1/x_{a-\frac{k+1}{2}} & \text{otherwise} \end{cases}
$$

and similarly for v:

$$
(4.9) \qquad \frac{v_{k-2,a-1} \, v_{k-2,a}}{v_{k-3,a-1} \, v_{k-1,a}} = \begin{cases} 1/y_{a-\frac{k}{2}} & \text{if } k \text{ even} \\ 1 & \text{otherwise} \end{cases}
$$

Let us pick i, j, k such that $i + j + k = 0 \bmod 2$, and use the result for the cross-ratios of (4.8-4.9) for $a = \frac{i-j+k}{2}$. Noting finally that

$$
\frac{\theta_{i+1,j,2k}\theta_{i-1,j,2k}}{\theta_{i,j,2k+1}\theta_{i,j,2k-1}} = \begin{cases} \frac{a_\alpha b_{\alpha-1}}{c_\alpha d_\alpha} & \text{if } \frac{i+j+2k}{2} \text{ even} \\ \frac{a_{\alpha-1} b_\alpha}{c_\alpha d_\alpha} & \text{otherwise} \end{cases} \quad \left(\alpha = \frac{i-j}{2} \right)
$$

$$
\frac{\theta_{i+1,j,2k-1}\theta_{i-1,j,2k-1}}{\theta_{i,j,2k}\theta_{i,j,2k-2}} = \begin{cases} \frac{c_\alpha d_{\alpha+1}}{a_\alpha b_\alpha} & \text{if } \frac{i+j+2k-1}{2} \text{ even} \\ \frac{c_{\alpha+1} d_\alpha}{a_\alpha b_\alpha} & \text{otherwise} \end{cases} \quad \left(\alpha = \frac{i-j-1}{2} \right)
$$

we conclude that

$$
L_{i,j,2k} = \begin{cases} \frac{a_\alpha b_{\alpha-1}}{a_\alpha b_{\alpha-1} + a_{\alpha-1} b_\alpha} & \text{if } i + j + 2k = 0 \bmod 4 \\ \frac{a_{\alpha-1} b_\alpha}{a_\alpha b_{\alpha-1} + a_{\alpha-1} b_\alpha} & \text{if } i + j + 2k = 2 \bmod 4 \end{cases} \quad \left(\alpha = \frac{i-j}{2} \right)
$$

$$
L_{i,j,2k-1} = \begin{cases} \frac{c_{\alpha+1} d_\alpha}{c_\alpha d_{\alpha+1} + c_{\alpha+1} d_\alpha} & \text{if } i + j + 2k - 1 = 0 \bmod 4 \\ \frac{c_\alpha d_{\alpha+1}}{c_\alpha d_{\alpha+1} + c_{\alpha+1} d_\alpha} & \text{if } i + j + 2k - 1 = 2 \bmod 4 \end{cases} \quad \left(\alpha = \frac{i-j-1}{2} \right)
$$

Similarly we compute the quantities:

$$
R_{i,j,2k} = \begin{cases} \frac{a_{\alpha-1}b_\alpha}{a_\alpha b_{\alpha-1}+a_{\alpha-1}b_\alpha} & \text{if } i+j+2k = 0 \bmod 4 \\ \frac{a_\alpha b_{\alpha-1}}{a_\alpha b_{\alpha-1}+a_{\alpha-1}b_\alpha} & \text{if } i+j+2k = 2 \bmod 4 \end{cases} \quad \left(\alpha = \frac{i-j}{2}\right)
$$

$$
R_{i,j,2k-1} = \begin{cases} \frac{c_\alpha d_{\alpha+1}}{c_\alpha d_{\alpha+1}+c_{\alpha+1}d_\alpha} & \text{if } i+j+2k-1 = 0 \bmod 4 \\ \frac{c_{\alpha+1}d_\alpha}{c_\alpha d_{\alpha+1}+c_{\alpha+1}d_\alpha} & \text{if } i+j+2k-1 = 2 \bmod 4 \end{cases} \quad \left(\alpha = \frac{i-j-1}{2}\right)
$$

We conclude that $R_{i,j,k}+L_{i,j,k}=1$ for all $k \geq 0$ and $i,j \in \mathbb{Z}$, and therefore $T_{i,j,k}$ satisfies the T-system (2.1). Moreover, the initial values of $T_{i,j,k}$ are $T_{i,j,i+j+1 \bmod 2} = \theta_{i,j,i+j+1 \bmod 2} = t_{i,j}$ by (4.6). The theorem follows. $\square$

Example 4.3. *For $m = 1$, all sequences are constant, $a_i = a$, $b_i = b$, $c_i = c$, $d_i = d$, and $x_i = \frac{2ab}{cd} = x$, $y_i = \frac{2cd}{ab} = y$. Moreover, we have $u_{n,i} = x^{\lfloor \frac{(n+1)^2}{4} \rfloor}$, $v_{n,i} = y^{\lfloor \frac{(n+1)^2}{4} \rfloor}$, hence:*

$$
T_{i,j,k} = 2^{\frac{k(k-1)}{2}} \left(\frac{ab}{cd}\right)^{\lfloor \frac{k}{2} \rfloor} \left\{ \delta_{k,0}^{[2]} \left(a\, \delta_{i+j+k,1}^{[4]} + b\, \delta_{i+j+k,3}^{[4]}\right) + \delta_{k,1}^{[2]} \left(c\, \delta_{i+j+k,1}^{[4]} + d\, \delta_{i+j+k,3}^{[4]}\right) \right\}
$$

and finally

$$
R_{i,j,k} = L_{i,j,k} = \frac{1}{2} \qquad (i,j \in \mathbb{Z}; k \in \mathbb{Z}_+; i+j+k = 0 \bmod 2)
$$

Example 4.4. *For $m = 2$, we find that*

$$
x_0 = \frac{c_1 d_0 + c_0 d_1}{a_0 b_0}, \quad x_1 = \frac{c_1 d_0 + c_0 d_1}{a_1 b_1}, \quad y_0 = \frac{a_0 b_1 + a_1 b_0}{c_0 d_0}, \quad y_1 = \frac{a_0 b_1 + a_1 b_0}{c_1 d_1}.
$$

and the solution reads:

$$
\begin{aligned}
T_{i,j,k} &= \delta_{k,0}^{[2]} \left(a_{\frac{i-j-1}{2}}\, \delta_{i+j+k,1}^{[4]} + b_{\frac{i-j-1}{2}}\, \delta_{i+j+k,3}^{[4]}\right) (x_0 x_1 y_0 y_1)^{\frac{k(k-2)}{8}} \left(x_{\frac{i-j-1}{2}}\right)^{\lfloor \frac{k+2}{4} \rfloor} \left(x_{\frac{i-j+1}{2}}\right)^{\lfloor \frac{k}{4} \rfloor} \\
&+ \delta_{k,1}^{[2]} \left(c_{\frac{i-j}{2}}\, \delta_{i+j+k,1}^{[4]} + d_{\frac{i-j}{2}}\, \delta_{i+j+k,3}^{[4]}\right) (x_0 x_1 y_0 y_1)^{\frac{k^2-1}{8}} \left(y_{\frac{i-j}{2}}\right)^{-\lfloor \frac{k-1}{4} \rfloor} \left(y_{\frac{i-j}{2}+1}\right)^{-\lfloor \frac{k+1}{4} \rfloor}
\end{aligned}
$$

4.2. **Density: exact derivation.** In this section we consider the T-system with m-toroidal boundary conditions. We define the density $\rho \equiv \rho^{(0,0)}$ as before as the response of the system to an infinitesimal perturbation of the initial data at position $(0,0)$, with value $T_{0,0,1} = t_{0,0} = c_0$. More precisely, we write:

$$
\rho_{i,j,k} = c_0 \frac{\partial \mathrm{Log}\, T_{i,j,k}}{\partial t_{0,0}} \bigg|_{t_{0,0}=c_0}
$$

Our aim in this section is to compute $\rho_{i,j,k}$ explicitly (As before, the singularity locus of the generating function for ρ will determine the suitable arctic curve.). Note that we have the following initial conditions:

(4.10) $\rho_{i,j,0} = 0$ and $\rho_{i,j,1} = \delta_{i,0}\delta_{j,0}$ $(i,j \in \mathbb{Z})$

Next, differentiating the T-system relation w.r.t. to $t_{0,0}$ provides us with the following system of linear recursion relations for $\rho_{i,j,k}$:

$$(4.11) \qquad \rho_{i,j,k+1} + \rho_{i,j,k-1} = L_{i,j,k}(\rho_{i+1,j,k} + \rho_{i-1,j,k}) + R_{i,j,k}(\rho_{i,j+1,k} + \rho_{i,j-1,k})$$

which, together with the initial conditions (4.10), determine $\rho_{i,j,k}$ entirely. The crucial remark here is that although this system is infinite, it has only finitely many distinct coefficients. Indeed, from Theorem 4.2, we deduce the following simple:

Corollary 4.5. *The quantities $(L_{i,j,k}, R_{i,j,k})$ for the solutions of the T-system with m-toroidal boundary conditions have the following periodicities:*

$$L_{i+2,j+2,k} = L_{i,j,k} \qquad L_{i+m,j-m,k} = L_{i,j,k} \qquad L_{i+1,j+1,k+2} = L_{i,j,k}$$
$$R_{i+2,j+2,k} = R_{i,j,k} \qquad R_{i+m,j-m,k} = R_{i,j,k} \qquad R_{i+1,j+1,k+2} = R_{i,j,k}$$

Proof. The first two relations are clear, as this periodicity is inherited from that of the initial data (4.1). The last one is checked directly on the expressions for $L_{i,j,k}, R_{i,j,k}$ of Theorem 4.2: one simply notices that the translation $(i, j, k) \to (i + 1, j + 1, k + 2)$ leaves α and β invariant, and leaves also the quantity $i + j + k \to i + j + k + 4$ invariant modulo 4, and $k \to k + 2$ invariant modulo 2. $\qquad\square$

In other words, coefficients of the system (4.11) are periodic in the $\mathbb{Z}^3$ lattice, with period vectors: $\vec{e}_1 = (2, 2, 0)$, $\vec{e}_2 = (m, -m, 0)$ and $\vec{e}_3 = (1, 1, 2)$. This suggests to introduce the following generating functions, for $i, j \in \mathbb{Z}$ and $k \in \mathbb{Z}_+$:

$$\rho^{(i,j,k)}(x, y, z) = \sum_{a,b\in\mathbb{Z},c\geq 0} \rho_{i+2a+mb+c,j+2a-mb+c,k+2c} x^{i+2a+mb+c} y^{j+2a-mb+c} z^{k+2c}$$

while the total density generating function $\rho(x, y, z) = \sum_{i,j\in\mathbb{Z},k\in\mathbb{Z}_+} x^i y^j z^k \rho_{i,j,k}$ is equal to the sum

$$\rho(x, y, z) = \sum_{(i,j,k)\in\Pi_m} \rho^{(i,j,k)}(x, y, z)$$

where Π_m is the set of integral points within the paralellepipedon based on $\vec{e}_i$, $i = 1, 2, 3$, namely:

$$\Pi_m = \{\sum_{i=1}^{3} t_i\vec{e}_i, \ 0 \leq t_i < 1\} \cap \{(i, j, k) \in \mathbb{Z}^3, \ i + j + k = 1 \bmod 2\}$$

Note that with the above definition, $\rho^{(i,j,k)}(x, y, z)$ is periodic in i, j, k, namely it satisfies:

$$\rho^{(i+2a+mb+c,j+2a-mb+c,k+2c)}(x, y, z) = \rho^{(i,j,k)}(x, y, z)$$

for $a, b \in \mathbb{Z}$ and $c \in \mathbb{Z}_+$, for all $i, j \in \mathbb{Z}$ and $k \in \mathbb{Z}_+$. For later use, we also note that, extending the above definition to $k = -1$ leads to:

$$
\begin{aligned}
\rho^{(i,j,-1)}(x,y,z) &= -z^{-1}\delta_{i,0}\delta_{j,0} + \sum_{a,b\in\mathbb{Z},c\geq 1} \rho_{i+2a+mb+c,j+2a-mb+c,k+2c} x^{i+2a+mb+c} y^{j+2a-mb+c} z^{k+2c} \\
&= -z^{-1}\delta_{i,0}\delta_{j,0} + \rho^{(i+1,j+1,1)}(x,y,z)
\end{aligned}
$$

where we have used $\rho_{i,j,1} + \rho_{i,j,-1} = 0$ and the initial condition. We finally obtain the following system for the generating functions $\rho^{(i,j,k)}(x,y,z)$, $k = 0, 1$ by use of the periodicities:

For $i + j = 0 \bmod 2$:
$$
\begin{aligned}
z^{-1}\rho^{(i,j,1)}(x,y,z) + z\rho^{(i+1,j+1,1)}(x,y,z) &= L_{i,j,0}(x^{-1}\rho^{(i+1,j,0)}(x,y,z) + x\rho^{(i-1,j,0)}(x,y,z)) \\
&\quad + R_{i,j,0}(y^{-1}\rho^{(i,j+1,0)}(x,y,z) + y\rho^{(i,j-1,0)}(x,y,z)) + \delta_{i,0}\delta_{j,0}
\end{aligned}
$$

For $i + j = 1 \bmod 2$:
$$
\begin{aligned}
z^{-1}\rho^{(i-1,j-1,0)}(x,y,z) + z\rho^{(i,j,0)}(x,y,z) &= L_{i,j,1}(x^{-1}\rho^{(i+1,j,1)}(x,y,z) + x\rho^{(i-1,j,1)}(x,y,z)) \\
&\quad + R_{i,j,1}(y^{-1}\rho^{(i,j+1,1)}(x,y,z) + y\rho^{(i,j-1,1)}(x,y,z))
\end{aligned}
$$

We may actually further restrict this system to a fundamental domain P_m of the (i, j, k), $k = 0, 1$ planes modulo $\vec{e}_1$ and $\vec{e}_2$, which we take to be:

$$
P_m = \Big\{ (i+1, -i, 0), (i+2, -i+1, 0), (i, -i, 1), (i+1, -i+1, 1) \Big\}_{i\in\{0,1,\ldots,m-1\}}
$$

Let us define the four following m-periodic functions for $i \in \mathbb{Z}$:

$$
\begin{aligned}
\alpha_i(x,y,z) &= \rho^{(i+1,-i,0)}(x,y,z), & \beta_i(x,y,z) &= \rho^{(i+2,-i+1,0)}(x,y,z) \\
\gamma_i(x,y,z) &= \rho^{(i,-i,1)}(x,y,z), & \delta_i(x,y,z) &= \rho^{(i+1,-i+1,1)}(x,y,z)
\end{aligned}
$$

and the coefficients

$$
(4.12) \qquad \lambda_i = L_{i,-i,0} = \frac{a_i b_{i-1}}{a_{i-1}b_i + a_i b_{i-1}} \qquad \mu_i = L_{i+2,-i+1,1} = \frac{c_{i+1}d_i}{c_i d_{i+1} + c_{i+1}d_i}
$$

so that $L_{i+1,-i+1,0} = 1 - \lambda_i$ and $L_{i+3,-i+2,1} = 1 - \mu_i$. Note also that, as is readily seen from their definition, these coefficients are not independent, as they must satisfy the relations:

$$
(4.13) \qquad \prod_{i=0}^{m-1} \left(\frac{1}{\lambda_i} - 1 \right) = \prod_{i=0}^{m-1} \left(\frac{1}{\mu_i} - 1 \right) = 1
$$

We may summarize the above results into:

Theorem 4.6. *The density generating functions $\alpha_i, \beta_i, \gamma_i, \delta_i$, for $i \in \{0, 1, ..., m-1\}$, are uniquely determined as the solutions of the following $4m \times 4m$ linear system:*

$$
\begin{aligned}
z^{-1}\,\alpha_i + z\,\beta_i - \lambda_i\,(x^{-1}\,\gamma_{i+1} + x\,\delta_i) - (1-\lambda_i)(y^{-1}\,\gamma_i + y\,\delta_{i+1}) &= 0 \\
z^{-1}\,\beta_i + z\,\alpha_i - (1-\lambda_i)(x^{-1}\,\delta_{i+1} + x\,\gamma_i) - \lambda_i\,(y^{-1}\,\delta_i + y\,\gamma_{i+1}) &= 0 \\
z^{-1}\,\gamma_i + z\,\delta_i - \mu_i\,(x^{-1}\,\alpha_i + x\,\beta_{i-1}) - (1-\mu_i)(y^{-1}\,\alpha_{i-1} + y\,\beta_i) &= \delta_{i,0} \\
(4.14) \qquad z^{-1}\,\delta_i + z\,\gamma_i - (1-\mu_i)(x^{-1}\,\beta_i + x\,\alpha_{i-1}) - \mu_i\,(y^{-1}\,\beta_{i-1} + y\,\alpha_i) &= 0
\end{aligned}
$$

for $i, j \in \{0, 1, ..., m-1\}$, subject to the periodicity conditions $\alpha_m = \alpha_0$, $\alpha_{-1} = \alpha_{m-1}$, and similarly for the β, γ, δ's.

The solution of the general system for the m-periodic densities of Theorem 4.6 is always a rational fraction of x, y, z, with denominator given by the determinant of the system (4.14). The matrix of coefficients may be rewritten in block form as:

$$
M = \begin{pmatrix}
z^{-1}I & zI & -M(x,y) & -\bar{M}(y^{-1},x^{-1}) \\
z\,I & z^{-1}I & -M(y^{-1},x^{-1}) & -\bar{M}(x,y) \\
-P(x,y) & -\bar{P}(y^{-1},x^{-1}) & z^{-1}I & z\,I \\
-\bar{P}(x,y) & -P(y^{-1},x^{-1}) & z\,I & z^{-1}I
\end{pmatrix}
$$

where all the entries are $m \times m$ matrices, with:

$$
P(x,y) = \begin{pmatrix}
\frac{\mu_0}{x} & 0 & 0 & \cdots & 0 & \frac{1-\mu_0}{y} \\
\frac{1-\mu_1}{y} & \frac{\mu_1}{x} & 0 & & & 0 \\
0 & \frac{1-\mu_2}{y} & \frac{\mu_2}{x} & \ddots & & 0 \\
\vdots & \ddots & \ddots & \ddots & \ddots & \vdots \\
\vdots & & \ddots & \ddots & \ddots & 0 \\
0 & \cdots & \cdots & 0 & \frac{1-\mu_{m-1}}{y} & \frac{\mu_{m-1}}{x}
\end{pmatrix}
$$

$$
M(x,y) = \begin{pmatrix}
\frac{1-\lambda_0}{y} & \frac{\lambda_0}{x} & 0 & \cdots & 0 & 0 \\
0 & \frac{1-\lambda_1}{y} & \frac{\lambda_1}{x} & \ddots & & 0 \\
0 & 0 & \frac{1-\lambda_2}{y} & \frac{\lambda_2}{x} & \ddots & \vdots \\
\vdots & \ddots & \ddots & \ddots & \ddots & 0 \\
0 & & \ddots & \ddots & \ddots & \frac{\lambda_{m-2}}{x} \\
\frac{\lambda_{m-1}}{x} & \cdots & \cdots & 0 & 0 & \frac{1-\lambda_{m-1}}{x}
\end{pmatrix}
$$

and $\bar{P}(x,y)$ is $P(x,y)$ with μ_i and $1-\mu_i$ interchanged, while $\bar{M}(x,y)$ is $M(x,y)$ with λ_i and $1-\lambda_i$ interchanged.

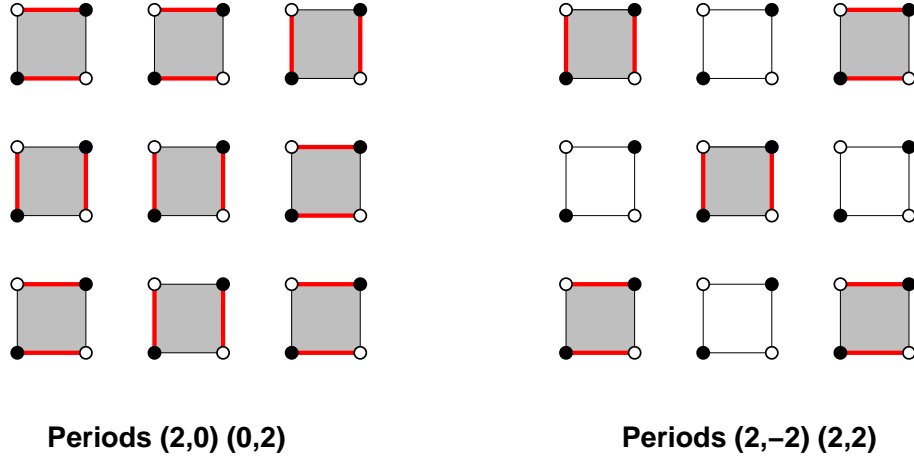**Periods (2,0) (0,2)**   **Periods (2,–2) (2,2)**

FIGURE 12. Comparison between the facet phases of the 2×2 (left) and 2-toroidal (right) T-system. In the latter the pinning of configurations for small c_0 is on a larger square sublattice (of c_0-type faces). But as a result, the sublattice of d_1-type faces decouples entirely, and these also have two arbitrary parallel dimer configurations, which makes the phases identical configurationwise.

Example 4.7. *For $m = 1$, the relation (4.13) gives $\lambda_0 = \mu_0 = \frac{1}{2}$ as expected. Moreover, denoting by $\alpha \equiv \alpha_0$, etc., the linear system of Theorem 4.6 reduces to:*

$$z^{-1} \alpha + z \beta - \frac{1}{2}(x^{-1} \gamma + x \delta) - \frac{1}{2}(y^{-1} \gamma + y \delta) = 0$$

$$z^{-1} \beta + z \alpha - \frac{1}{2}(x^{-1} \delta + x \gamma) - \frac{1}{2}(y^{-1} \delta + y \gamma) = 0$$

$$z^{-1} \gamma + z \delta - \frac{1}{2}(x^{-1} \alpha + x \beta) - \frac{1}{2}(y^{-1} \alpha + y \beta) = 1$$

$$z^{-1} \delta + z \gamma - \frac{1}{2}(x^{-1} \beta + x \alpha) - \frac{1}{2}(y^{-1} \beta + y \alpha) = 0$$

The total density $\rho = \alpha + \beta + \gamma + \delta$ therefore satisfies:

$$\left(z^{-1} + z - \frac{1}{2}(x + x^{-1} + y + y^{-1})\right)\rho(x, y, z) = 1$$

which matches (2.12).

Example 4.8. *For $m = 2$, the relation (4.13) gives $\lambda_1 = 1 - \lambda_0$ and $\mu_1 = 1 - \mu_0$. The 8×8 linear system of Theorem 4.6 reads:*

$$
\begin{aligned}
z^{-1}\alpha_0 + z\beta_0 - \lambda_0\,(x^{-1}\gamma_1 + x\,\delta_0) - \lambda_1\,(y^{-1}\gamma_0 + y\,\delta_1) &= 0 \\
z^{-1}\beta_0 + z\alpha_0 - \lambda_1\,(x^{-1}\delta_1 + x\,\gamma_0) - \lambda_0\,(y^{-1}\delta_0 + y\,\gamma_1) &= 0 \\
z^{-1}\alpha_1 + z\beta_1 - \lambda_1\,(x^{-1}\gamma_0 + x\,\delta_1) - \lambda_0\,(y^{-1}\gamma_1 + y\,\delta_0) &= 0 \\
z^{-1}\beta_1 + z\alpha_1 - \lambda_0\,(x^{-1}\delta_0 + x\,\gamma_1) - \lambda_1\,(y^{-1}\delta_1 + y\,\gamma_0) &= 0 \\
z^{-1}\gamma_0 + z\delta_0 - \mu_0\,(x^{-1}\alpha_0 + x\,\beta_1) - \mu_1\,(y^{-1}\alpha_1 + y\,\beta_0) &= 1 \\
z^{-1}\delta_0 + z\gamma_0 - \mu_1\,(x^{-1}\beta_0 + x\,\alpha_1) - \mu_0\,(y^{-1}\beta_1 + y\,\alpha_0) &= 0 \\
z^{-1}\gamma_1 + z\delta_1 - \mu_1\,(x^{-1}\alpha_1 + x\,\beta_0) - \mu_0\,(y^{-1}\alpha_0 + y\,\beta_1) &= 0 \\
z^{-1}\delta_1 + z\gamma_1 - \mu_0\,(x^{-1}\beta_1 + x\,\alpha_0) - \mu_1\,(y^{-1}\beta_0 + y\,\alpha_1) &= 0
\end{aligned}
$$

This boils down to the following 4×4 system for a new set of generating functions: $\alpha = \alpha_0 + \beta_1$, $\beta = \beta_0 + \alpha_1$, $\gamma = \gamma_0 + \delta_1$ and $\delta = \delta_0 + \gamma_1$:

$$
\begin{aligned}
z^{-1}\alpha + z\beta - \lambda_0\,(x^{-1} + x)\delta - \lambda_1\,(y^{-1} + y)\gamma &= 0 \\
z^{-1}\beta + z\alpha - \lambda_1\,(x^{-1} + x)\gamma - \lambda_0\,(y^{-1} + y)\delta &= 0 \\
z^{-1}\gamma + z\delta - \mu_0\,(x^{-1} + x)\alpha - \mu_1\,(y^{-1} + y)\beta &= 1 \\
z^{-1}\delta + z\gamma - \mu_1\,(x^{-1} + x)\beta - \mu_0\,(y^{-1} + y)\alpha &= 0
\end{aligned}
$$

with $\lambda_0 + \lambda_1 = 1 = \mu_0 + \mu_1$. Note that this system is equivalent to that of (3.4), with $\lambda_1 = \sigma$ and $\mu_1 = \tau$. The simple reason for this is that the condition (4.13) has induced a more restrictive periodicity condition on the coefficients λ_i, μ_i, namely $\lambda_1 = 1 - \lambda_0$ and $\mu_1 = 1 - \mu_0$, which is equivalent to that of Section 3. Another indication is found by comparing the facet phases in both models. We have represented in Fig.12 the two facet phases. The pinning of dimer configurations on c_0 type faces for c_0 small induces a pinning on d_1 faces as well, which makes the two phases identical.

4.3. **Arctic curves and phase diagram.** It is clear that the solution of the general system for the m-periodic densities of Theorem 4.6 is always a rational fraction of x, y, z, with denominator given by the determinant of the system (4.14). Applying the usual analysis to the singularity locus of this denominator yields some algebraic arctic curve of higher degree. The details being cumbersome, we display here various plots of these curves for $m = 3, 4$.

4.3.1. *Case $m = 3$.* For $m = 3$, the arctic curve is found generically to be the zero locus of a polynomial of degree 14 in u, v. In the physical range of parameters $\lambda_i, \mu_i \in [0, 1]$, we find generically 3 disconnected pieces, a first curve tangent to the square $|u| + |v| = 1$ in four points, and two inner pieces, each with 4 cusps, thus defining three inner regions in addition to the 4 frozen corners. As before, we expect the two innermost regions to correspond to facet type phases, where the configurations get pinned to the faces with the
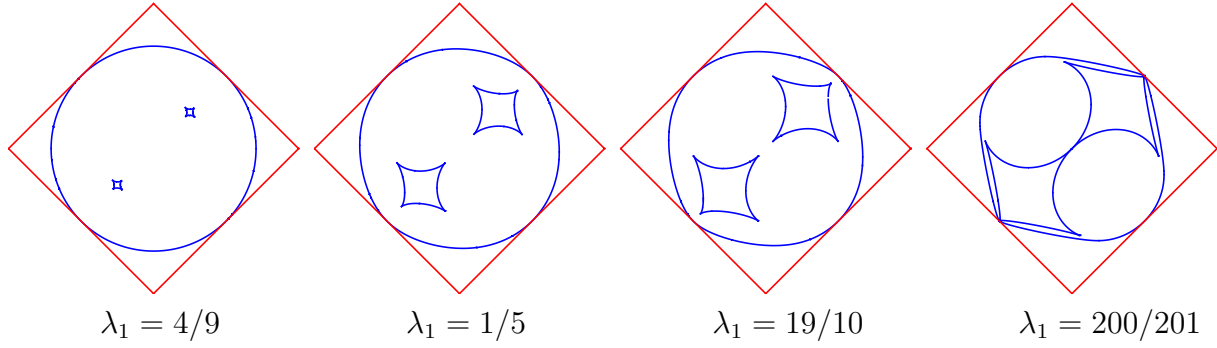
$$\lambda_1 = 4/9 \qquad \lambda_1 = 1/5 \qquad \lambda_1 = 19/10 \qquad \lambda_1 = 200/201$$

FIGURE 13. Arctic curves for the 3-toroidal initial data corresponding to different values of λ_1. Where $\lambda_0 = 1/2$, $\lambda_2 = 1 - \lambda_1$ and $\mu_0 = \mu_1 = \mu_2 = 1/2$.

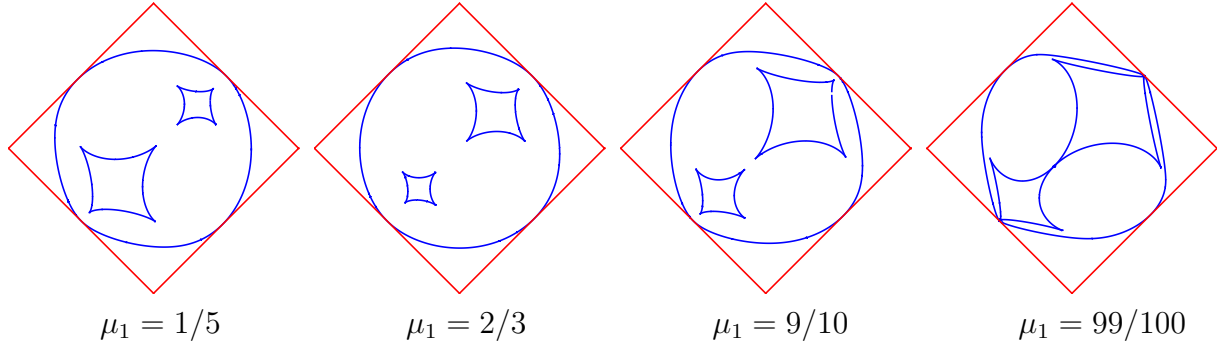$$\mu_1 = 1/5 \qquad \mu_1 = 2/3 \qquad \mu_1 = 9/10 \qquad \mu_1 = 99/100$$

FIGURE 14. Arctic curves for the 3-toroidal initial data corresponding to different values of μ_1. Where $\lambda_0 = 1/2$, $\lambda_1 = 1/4$, $\lambda_2 = 1 - \lambda_1 = 3/4$, $\mu_0 = 1/2$ and $\mu_2 = 1 - \mu_1$.

smallest weights. As before, the density tends to 0 exponentially in the corners, and as a power of k in the disordered region.

Assuming say that $c_0 \to 0$ while the other faces weights remain finite, we expect the crystalline state depicted in Fig.15 (a) to be dominant, while if $c_0 \sim d_1 \to 0$, the crystalline state of Fig.15 (b) tends to dominate the partition function. We have a pinning of the configurations on the shaded faces with small weights, all tending to be occupied by two parallel dimers, with 2 possibilities on each shaded face.

These however are not compatible with the boundary conditions of the Aztec graph, hence the formation of facets. Note that no facet occupies the center of the Aztec graph. In the extreme case when one of the weights tends to 0 (see Fig.14 right, with $\mu_1 = \frac{99}{100}$, $\mu_2 = \frac{1}{100}$), the two facets meet at a quadruple point in the center, which in the limit is the intersection of two tangent ellipses).
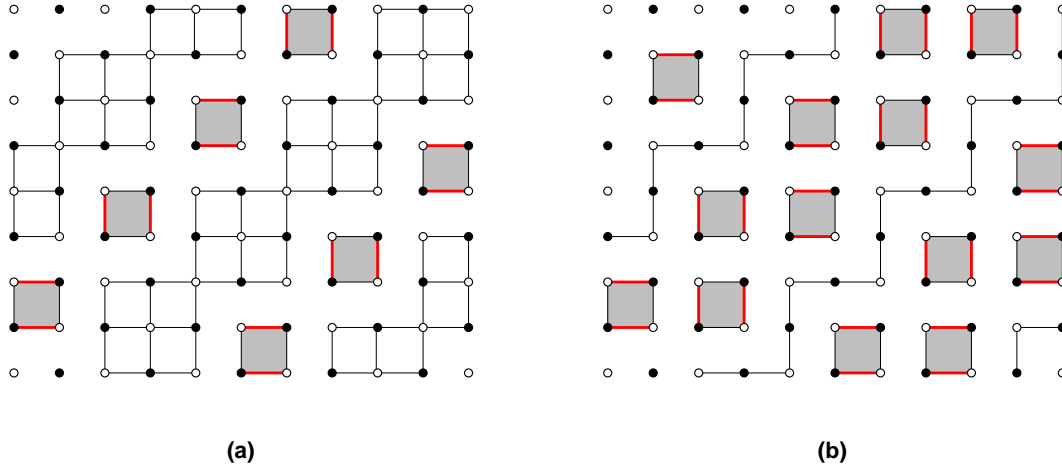
(a)   (b)

FIGURE 15. Typical dominant states for the 3-toroidal partition function, in the cases where: (a) $c_0 \to 0$ while all other face weights remain finite (we have shaded the c_0-type faces); and (b) $c_0 \sim d_1 \to 0$ while all other face weights remain finite (both types of faces are shaded).

$\mu_0 = 5/9(c_0 = 4/5)$ $\mu_0 = 3/5(c_0 = 2/3)$ $\mu_0 = 4/5(c_0 = 1/4)$ $\mu_0 = 9/10(c_0 = 1/9)$
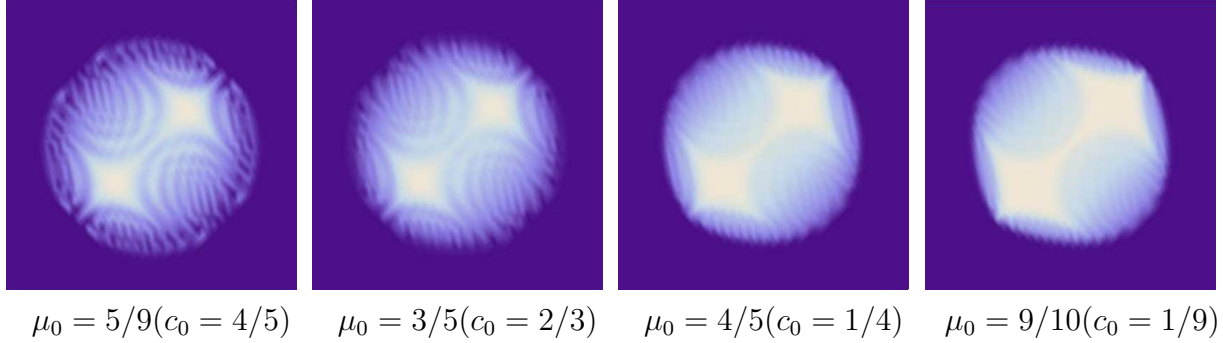
FIGURE 16. Density profiles for $\rho_{i,j,k}$ for the 3-toroidal initial data corresponding to different values of μ_0. Where $\mu_1 = 1/2$, $\mu_2 = 1 - \mu_0$ and $\lambda_0 = \lambda_1 = \lambda_2 = 1/2$. (We have fixed $a_0 = a_1 = a_2 = b_0 = b_1 = b_2 = c_1 = c_2 = d_0 = d_1 = d_2 = 1$ and only vary c_0.)

We have displayed in Fig. 13 the arctic curves occurring when the μ parameters are all trivial ($= 1/2$) while the λ's vary. The curve is symmetric, and the two facets have identical size. In Fig.14 however, we have let both λ's and μ's vary, and we see that the relative sizes of the facets vary as well. The qualitative explanation for this is that one of the facet phases is more compatible with certain corners than others.

Like in the 2×2 periodic initial data case of Sect.3.4.2, the behavior of $\rho_{i,j,k}$ for large k is found by comparing how the numerator and denominator of the expression for $\rho^{(0,0)}(x, y, z)$
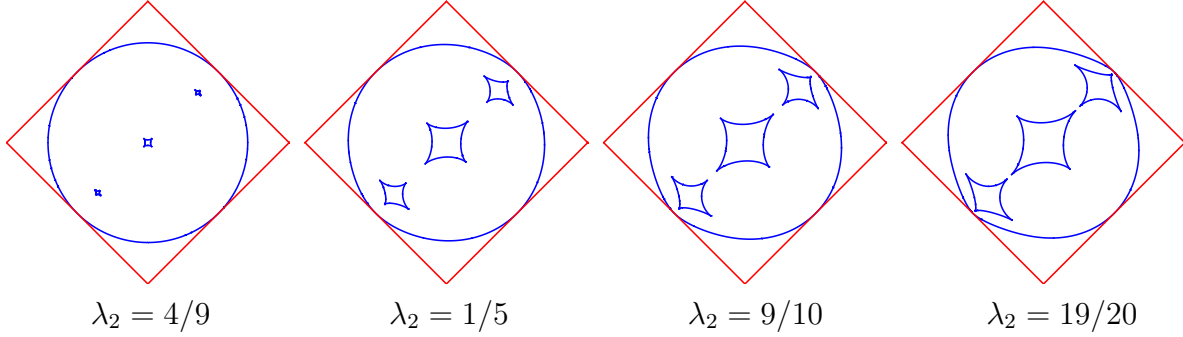
$$\lambda_2 = 4/9 \qquad \lambda_2 = 1/5 \qquad \lambda_2 = 9/10 \qquad \lambda_2 = 19/20$$

FIGURE 17. Arctic curves for the 4-toroidal initial data corresponding to different values of λ_2. Where $\lambda_0 = 1/2$, $\lambda_1 = 1/2$, $\lambda_3 = 1 - \lambda_2$ and $\mu_0 = \mu_1 = \mu_2 = \mu_3 = 1/2$.

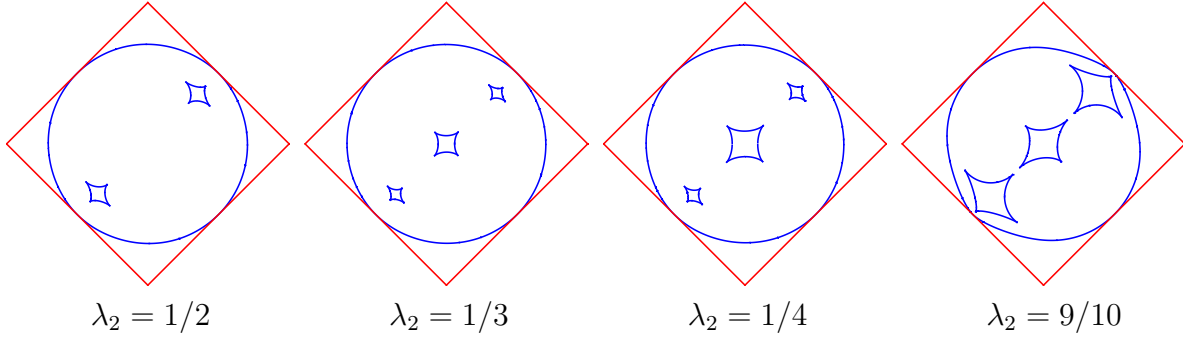$$\lambda_2 = 1/2 \qquad \lambda_2 = 1/3 \qquad \lambda_2 = 1/4 \qquad \lambda_2 = 9/10$$

FIGURE 18. Arctic curves for the 4-toroidal initial data corresponding to different values of λ_2. Where $\lambda_0 = 1/2$, $\lambda_1 = 2/3$, $\lambda_3 = \frac{2}{1+\lambda_2} - 1$ and $\mu_0 = \mu_1 = \mu_2 = \mu_3 = 1/2$.

behave in the vicinity of the singular point $x = y = z = 1$. We find that $\rho^{(0,0)}(1 - tx, 1 - ty, 1 - tz)$ behaves as t^{-3} when $\lambda_0 \neq \lambda_2$, and as t^{-2} otherwise, which means that if $\lambda_0 \neq \lambda_2$ $\rho_{i,j,k}$ tends to 0 algebraically as k^{-1}, whereas it goes to a scaling function without overall scaling otherwise. We have represented the profiles of the density function $k\rho_{i,j,k}^{(0,0)}$ for size $k = 77$ in Fig.16.

4.3.2. *Case $m = 4$.* The structure of phases is similar to the cases $m = 2, 3$, except that we now have 3 inner facet regions along the diagonal of the square domain. As before, we first display in Figs.17-18 the case when all μ's are trivial ($= 1/2$) and λ's vary. We see that the picture is again symmetric w.r.t. the center. In Fig. 19, we let both λ's and μ's vary, and observe that the relative sizes of the various facet regions vary.

Note finally that the case $m = 4$ reduces to the case $m = 2$ if we choose $\lambda_2 = \lambda_0$ and $\lambda_3 = \lambda_1 = 1 - \lambda_0$, and $\mu_2 = \mu_0$, $\mu_3 = \mu_1 = 1 - \mu_0$, as this changes the periodicity of $R_{i,j,k}$, $L_{i,j,k}$ to $\vec{e_1}' = (2,2)$, $\vec{e_2}' = (2,-2)$ and $\vec{e_3}' = (1,1,2)$.

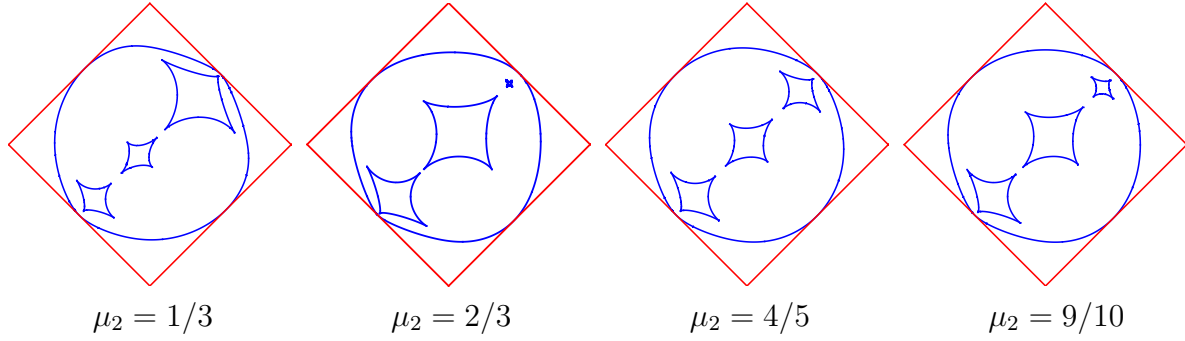$$\mu_2 = 1/3 \qquad \mu_2 = 2/3 \qquad \mu_2 = 4/5 \qquad \mu_2 = 9/10$$

FIGURE 19. Arctic curves for the 4-toroidal initial data corresponding to different values of μ_2. Where $\lambda_0 = 1/2$, $\lambda_1 = 2/3$, $\lambda_2 = 4/5$, $\lambda_3 = 1/9$ and $\mu_0 = 1/2$, $\mu_1 = 1/4$ and $\mu_3 = \frac{3(1-\mu_2)}{3-2\mu_2}$.
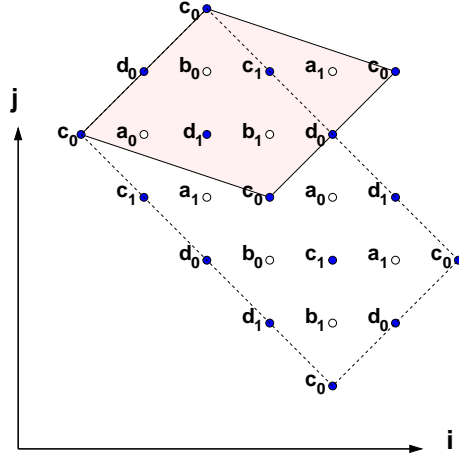

FIGURE 20. For the 4-toroidal case with $\lambda_0 + \lambda_2 = \lambda_1 + \lambda_3 = 1$ and $\mu_0 + \mu_2 = \mu_1 + \mu_3 = 1$, the fundamental domain is *de facto* reduced by half. We have shaded the new fundamental domain, generated by $(2,2)$ and $(3,-1)$.

Another interesting sub-case is when $\lambda_0 + \lambda_2 = \lambda_1 + \lambda_3 = 1$ while $\mu_0 + \mu_2 = \mu_1 + \mu_3 = 1$. In this case, we get a family of curves with one less facet region, which qualitatively look like those of the $m = 3$ case (see Fig.18 left for an example with $\lambda_0 = \frac{1}{2}$ and $\lambda_1 = \frac{2}{3}$ while $\mu_0 = \mu_1 = \frac{1}{2}$). Note that the choice of parameters above has changed the periodicity of $R_{i,j,k}$, $L_{i,j,k}$ to $\vec{e_1}' = (2,2)$, $\vec{e_2}' = (3,-1)$ and $\vec{e_3}' = (1,1,2)$, thus effectively dividing by 2 the volume of the fundamental domain in $\mathbb{Z}^3$ for the 4-toroidal case. One way of realizing the relations between the λ's and the μ's is to take $c_{i+2} = d_i$, $d_{i+2} = c_i$ and $b_{i+2} = a_i$, $a_{i+2} = b_i$ for all i. The torus of initial data in this case is twice as small, generated by $(2,2)$ and $(3,-1)$ as shown in Fig.20.

Note that despite its qualitative similarity with the $m = 3$ case, this is different, as the two fundamental domains are inequivalent.

4.3.3. *General case and quotients.* In general, we expect generically $m - 1$ facet regions along the diagonal of the square $|u| + |v| = 1$. Like in the cases $m = 2, 3, 4$, we find that $\rho^{(0,0)}(1 - tx, 1 - ty, 1 - tz)$ behaves like t^{-3} for $\lambda_0 \neq \lambda_{m-1}$ and like t^{-2} otherwise, hence we expect that $\rho_{i,j,k}$ scales like k^{-1} for $\lambda_0 = \lambda_{m-1}$ and tends directly to a scaling function without overall rescaling otherwise.

For even $m = 2p$, we have, like for $m = 4$, two sub-cases of interest.

The first one is a reduction to the p-toroidal case, by picking parameters λ_i, μ_i such that $\lambda_{i+p} = \lambda_i$ and $\mu_{i+p} = \mu_i$ for $i = 0, 1, .., p - 1$. The second is by picking $\lambda_{i+p} = 1 - \lambda_i$ and $\mu_{i+p} = 1 - \mu_i$, $i = 0, 1, ..., p - 1$. The new periodicity of $R_{i,j,k}$, $L_{i,j,k}$ is $\vec{e_1}' = (2, 2)$, $\vec{e_2}' = (p + 1, p - 1)$ and $\vec{e_3}' = (1, 1, 2)$, again dividing by 2 the volume of the fundamental domain of $\mathbb{Z}^3$ of the m-toroidal case. For this reason, we call the corresponding boundary conditions the $\mathbb{Z}_2$ quotient of the $m = 2p$-toroidal case.

More generally, if $m = aq$ for some positive integers a, q, we may take $\lambda_{i+q} = \lambda_i$ and $\mu_{i+q} = \mu_i$ for all i to reduce the m-toroidal case to the q-toroidal one. Similarly, for $a = 2b$ even, picking $\lambda_{i+q} = 1 - \lambda_i$ and $\mu_{i+q} = 1 - \mu_i$, for all i reduces the m-toroidal case to one with periodicities $\vec{e_1}' = (2, 2)$, $\vec{e_2}' = (q + 1, q - 1)$ and $\vec{e_3}' = (1, 1, 2)$, that is to the $\mathbb{Z}_2$ quotient of the $2q$-toroidal case.

5. CONCLUSION AND DISCUSSION

5.1. **Summary and perspectives.** In this paper we have obtained the exact solutions of the octahedron equation with initial data satisfying m-toroidal boundary conditions, namely some specific doubly periodic initial conditions. We have used this solution to compute a density function of the associated dimer model on an Aztec graph, and investigate its singularities in the limit of large size of the graph.

The generic result is a phase diagram with three types of phases for the dimer configurations: frozen corners with no entropy, disordered intermediate region, and facets with order and entropy.

Our analysis uses exclusively the octahedron equation and the properties of its particular solutions. Analogous equations have been considered recently such as the cube recurrence [5] related to combinatorial groves and the hexahedron equation related to double-dimers [28]. Although not directly related to a dimer model, these display the same arctic phenomena [32, 28]. It would be interesting to see whether analogous exact solutions such as the m-toroidal ones of the present paper, exist in these other cases. If so, we expect some special patterns of frozen, disordered and facet phases to occur.

Another direction of generalization would consist of considering different geometries of initial data. In [11], arbitrary initial data on stepped surfaces for the octahedron equation
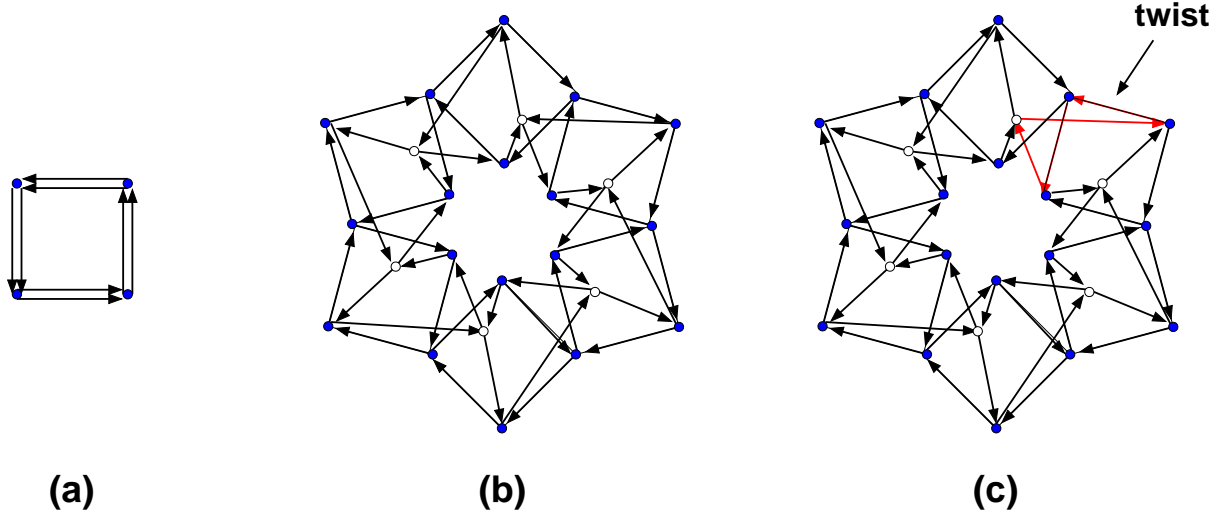
FIGURE 21. The quivers obtained by folding the T-system quiver onto a torus, for the 2×2 case (a), the $m = 6$-toroidal case (b) and the $\mathbb{Z}_2$ quotient of the $m = 12$-toroidal case (the quiver is simply obtained from the $m = 6$ case by a twist, i.e. reversal of 4 arrows as indicated).

were investigated. Given a stepped surface $(i, j, k_{i,j})_{i,j \in \mathbb{Z}}$ with $|k_{i,j+1} - k_{i,j}| = |k_{i+1,j} - k_{i,j}| = 1$ and $i + j + k_{i,j} = 1 \bmod 2$ for all i, j, these consist of the following initial data assignments:

$$T_{i,j,k_{i,j}} = t_{i,j} \qquad (i, j \in \mathbb{Z})$$

for some fixed parameters $t_{i,j}$, $i, j \in \mathbb{Z}$. It was shown in [11] that the solution $T_{i,j,k}$ of the octahedron equation with such initial conditions is the partition function of a dimer model on a graph obtained by taking the *shadow* of the point (i, j, k) onto the initial data surface, and attaching to the resulting graph edges weights expressed in terms of the local parameters $t_{i,j}$. We may now consider the succession of partition functions $T_{i,j,k}$ for domains of growing size as k increases. For sufficiently nice surfaces such as "flat" periodic structures with a fixed average rational normal vector, we expect the thermodynamic limit $k \to \infty$ of these models to make sense. Special solutions of the octahedron equation should still be amenable to the study of arctic curve phenomena. The same could possibly hold for the so-called brane tiling models [23].

5.2. **Cluster algebra and arctic curves.** The T-system equation is known to be a particular mutation in an infinite rank cluster algebra, with quiver given by an antiferromagnetic orientation of the edges of the square lattice $\mathbb{Z}^2$, namely such that every other square face is oriented clockwise. The cluster algebra describes rational transformations (called mutations) of variables (x_i) attached to the vertices i of the quiver as follows. There is a

mutation μ_k for each vertex k of the quiver, and the action of μ_k on (x_i) is [18]:

$$
\begin{aligned}
\mu_k(x_i) &= x_i \qquad \text{if } i \neq k \\
\mu_k(x_k) &= \frac{1}{x_k}\left(\prod_{i \to k} x_i + \prod_{k \to j} x_j\right)
\end{aligned}
$$

(5.1)

where the first product is over all the tails of arrows with head k, and the second is over all heads of arrows whose tail is k. The quiver mutates under μ_k as well (see [18] for a precise definition: this is a so-called cluster algebra of geometric type, without coefficients).

The doubly periodic situation we have investigated in this paper corresponds to finite rank *folded* cluster algebras, for which the above quiver has been folded, by identifying the vertices modulo the corresponding torus generators. We have represented in Fig.21 (a) the folded quiver for the 2×2 periodic case of Section 3, in Fig.21 (b) the folded quiver for the $m = 6$-toroidal case, and in in Fig.21 (c) the folded quiver for the $\mathbb{Z}_2$ quotient of the $m = 12$-toroidal case. The latter is obtained from the $m = 6$ quiver via a twist, namely the reversal of 4 arrows connecting two neighboring pairs of vertices. Alternatively, if we view the m-toroidal case quiver as a ribbon made of m oriented octahedra, then the $\mathbb{Z}_2$ quotient of the $2m$-toroidal case quiver is the corresponding Möbius strip. Note that all the quivers are naturally bi-partite.

The corresponding T system with toroidal boundary conditions is simply obtained by restricting to compound mutations in which one performs all mutations at vertices of a given parity, and alternating between the two parities (any such compound mutation reflects all the arrows of the quiver). Let us denote by $(x_i)_{i \in I}$ and $(B_{i,j})_{i,j \in I}$ respectively the cluster variables and exchange matrix elements coding the quiver (B is a skew-symmetric integer matrix, such that $B_{i,j} > 0$ counts the number of arrows from vertex i to j). Here I is a finite set, for instance $I = \{1, 2, ..., 4m\}$ in the m-toroidal case.

The special property of the above quivers and their compound mutations is that the "coefficient" variables defined as

(5.2)
$$
y_i = \prod_{k \in I} x_k^{B_{i,k}} \qquad (i \in I)
$$

take only finitely many distinct values under arbitrary compound mutations. Indeed, in all cases, we may identify y_i with the ratio $L_{i,j,k}/R_{i,j,k}$, which indeed takes only finitely many distinct values. Let us call *y-finite* the corresponding cluster algebra.

This property was instrumental for determining the density ρ exactly. More generally, we may define an analogue of such a density for any cluster algebra. Pick an initial cluster $(x_i)_{i \in I}$, and a particular cluster variable, say x_{i_0}. For any mutated cluster $(x'_i)_{i \in I}$ we may define the density:

$$
\rho^{(i_0)}(x'; x)_j = x_{i_0} \partial_{x_{i_0}} \log x'_j
$$

It is easy to derive a linear recursion relation for ρ_j by differentiating the mutation relation (5.1). We get:

$$\rho'_k + \rho_k = L \sum_{i \to k} \rho_i + R \sum_{k \to j} \rho_j$$

with $L/R = y_k$ and $L + R = 1$.

Assume that we choose some special set of (possibly compound) mutations, such that the variables y_i only take finitely many values under iteration of these mutations, then we see that ρ can be determined as the solution of a periodic linear system, with initial data $\rho^{(i_0)}(x; x)_j = \delta_{j,i_0}$. Denoting by $x^{(k)}$ the image of x under the k-th iterate of these mutations we may form the generating series: $\rho(\{w_i\}_{i \in I}; z) = \sum_{k \geq 0, j \in I} \rho^{(i_0)}(x^{(k)}; x)_j \, w_j \, z^k$. As $\rho^{(i_0)}(x^{(k)}; x)_j$ solve a periodic linear system, the function $\rho(\{w_i\}_{i \in I}; z)$ is necessarily a rational fraction of w_i, z. The denominator of this fraction governs the singularities of $\rho(\{w_i\}_{i \in I}; z)$ at large k. The interesting case is if I is infinite, and x_i doubly or multiply periodic, say $I = \{\vec{a} = (a_1, a_2, ..., a_r) \in \mathbb{Z}^r\}$ and $x_{\vec{a} + \vec{e}_i} = x_{\vec{a}}$ for r linearly independent vectors $\vec{e}_i$, $i = 1, 2, ..., r$. Then we can choose finitely many catalytic variables say $w_1, ..., w_r$ for the generating function $\rho(\{w_i\}_{i \in [1,r]}; z) = \sum_{k \geq 0, \vec{a} \in \mathbb{Z}^r} \rho^{(i_0)}(x^{(k)}; x)_{\vec{a}} \, w_{\vec{a}} \, z^k$ where $w_{\vec{a}} = \prod_{i=1}^r w_i^{a_i}$. This multivariate generating function will display an arctic curve, obtained by blowing up the vicinity of the point $w_i = 1$, $z = 1$.

This makes the search for y-finite cluster algebras worthwhile, as each of them will lead to interesting algebraic "arctic" curves.

REFERENCES

[1] I. Assem, C. Reutenauer and D. Smith, *Friezes*, Adv. Math. **225** (2010), 3134–3165. `arXiv:0906.2026` `[math.RA]`.

[2] Y. Baryshnikov and R. Pemantle. *Asymptotics of multivariate sequences, part III: quadratic points*, Advances in Mathematics **228** (2011) 3127-3206. `arXiv:0810.4898` `[math.CO]`.

[3] F. Bergeron and C. Reutenauer , SL_k-*Tiling of the Plane*, Illinois J. Math. **54** (2010), 263–300. `arXiv:1002.1089` `[math.CO]`.

[4] D. Bressoud, *Proofs and confirmations: The story of the alternating sign matrix conjecture*, MAA Spectrum, Mathematical Association of America, Washington, DC (1999), 274 pages.

[5] G. Carroll and D. Speyer, *The cube recurrence*, Elec. Jour. of Comb. Vol. **11** (2004) R73. `arXiv:math/0403417` `[math.CO]`.

[6] H. Cohn, N. Elkies, and J. Propp, *Local statistics for random domino tilings of the Aztec diamond*, Duke Math. J. Vol. **85**, Number 1 (1996), 117-166. `arXiv:math/0008243` `[math.CO]`.

[7] F. Colomo, V. Noferini, and A. G. Pronko, *Algebraic arctic curves in the domain-wall six-vertex model*, J. Phys. A: Math. Theor. **44(19)** (2011) 195201. `arXiv:1012.2555` `[math-ph]`.

[8] H.S.M. Coxeter, *Frieze Patterns, Triangulated Polygons and Dichromatic Symmetry*, in *The Lighter Side of Mathematics*, R.K. Guy and E. Woodrow (eds.), John Wiley & Sons, NY, (1961) pp 15-27.

[9] P. Di Francesco, *The solution of the A_r T-system for arbitrary boundary*, Elec. Jour. of Comb. Vol. **17(1)** (2010) R89. `arXiv:1002.4427` `[math.CO]`.

[10] P. Di Francesco, *An Inhomogeneous Lambda-determinant* Elec. Jour. of Comb. Vol. **20(3)** (2013) P19. `arXiv:1209.6619` `[math.CO]`.

[11] P. Di Francesco, *T-system, networks and dimers*, to appear in Comm. Math. Phys. (2014), `arXiv:1307.0095 [math-ph]`.

[12] P. Di Francesco and R. Kedem, *Q-systems as cluster algebras II*, Lett. Math. Phys. **89** No 3 (2009) 183-216. `arXiv:0803.0362 [math.RT]`.

[13] P. Di Francesco and R. Kedem, *Positivity of the T-system cluster algebra*, Elec. Jour. of Comb. Vol. **16(1)** (2009) R140, Oberwolfach preprint OWP 2009-21, `arXiv:0908.3122 [math.CO]`.

[14] P. Di Francesco and R. Kedem, *The solution of the quantum A_1 T-system for arbitrary boundary*, Comm. Math. Phys. **313**, No 2, (2012) 329–350. `arXiv:1102.5552 [math-ph]`.

[15] P. Di Francesco and R. Kedem, *T-system with boundaries from network solutions*, Elec. Jour. of Comb. Vol. **20(1)** (2013) P3. `arXiv:1208.4333 [math.CO]`.

[16] C. Dodgson, *Condensation of determinants*, Proceedings of the Royal Soc. of London **15** (1866) 150–155.

[17] N. Elkies, G. Kuperberg, M. Larsen and J. Propp, *Alternating sign matrices and domino tilings* (Parts I and II), Journal of Algebraic Combinatorics **1**, 111–132, 219–234 (1992). `arXiv:math/9201305 [math.CO]`.

[18] S. Fomin and A. Zelevinsky Cluster Algebras I. J. Amer. Math. Soc. **15** (2002), no. 2, 497–529 `arXiv:math/0104151 [math.RT]`.

[19] M. Gekhtman, M. Shapiro, S. Tabachnikov, and A. Vainshtein, Higher pentagram maps, weighted directed networks, and cluster dynamics, Electron. Res. Announc. Math. Sci., **19** (2012) 1–17. `arXiv:1110.0472 [math.QA]`.

[20] M. Glick, *The pentagram map and Y-patterns*, Adv. Math., **227** (2011) 1019–1045. `arXiv:1005.0598 [math.CO]`.

[21] A. B. Goncharov and R. Kenyon, *Dimers and cluster integrable systems*, Ann. Sci. ENS **46**, fascicule 5 (2013), 747–813. `arXiv:1107.5588 [math.AG]`.

[22] A. Henriques , *A periodicity theorem for the octahedron recurrence*, Jour. of Alg. Comb. Vol. **26** Issue 1 (2007),1–26. `arXiv:math/0604289 [math.CO]`.

[23] I.-J. Jeong, G. Musiker and S, Zhang, *Gale-Robinson Sequences and Brane Tilings*, proceedings of FPSAC 2013 Paris, France, DMTCS proc. AS, 2013, 73–748.

[24] W. Jockush, J. Propp and P. Shor *Random Domino Tilings and the Arctic Circle Theorem* `arXiv:math/9801068 [math.CO]`

[25] R. Kedem and P. Vichitkunakorn, *T-systems and the pentagram map*, preprint (2014).

[26] R. Kenyon and A. Okounkov, *Limit shapes and the complex Burgers equation*, Acta Math. Vol. **199**, No. 2 (2007), 263–302. `arXiv:math-ph/0507007`; *Planar dimers and Harnack curves*, Duke Math. J. Vol. **131**, No. 3 (2006), 499–524. `arXiv:math/0311062 [math.AG]`

[27] R. Kenyon, A. Okounkov and S. Sheffield, *Dimers and Amoebae*, Ann. Math. **163** (2006), no. 3, 1019–1056. `arXiv:math-ph/0311005`.

[28] R. Kenyon and R. Pemantle, *Double-dimers, the Ising model and the hexahedron recurrence*, proceedings of FPSAC 2013 Paris, France, DMTCS proc. AS, 2013, 141–152. `arXiv:1308.2998 [math-ph]`

[29] A. Knutson, T. Tao, and C. Woodward, *A positive proof of the Littlewood-Richardson rule using the octahedron recurrence*, Electr. J. Combin. **11** (2004) RP 61. `arXiv:math/0306274 [math.CO]`

[30] A. Kuniba, A. Nakanishi and J. Suzuki, *Functional relations in solvable lattice models. I. Functional relations and representation theory.* International J. Modern Phys. A **9** no. 30, pp 5215–5266 (1994). `arXiv:hep-th/9310060`.

[31] A. Kuniba, A. Nakanishi and J. Suzuki, *T-systems and Y-systems in integrable systems.* J. Phys. A: Mathematical and Theoretical, **44**(10) (2011) 103001. `arXiv:1010.1344 [hep-th]`

[32] T. Kyle-Petersen and D. Speyer, *An arctic circle theorem for Groves*, Jour. of Comb. Theory Ser. A **111** (2005) 137–164. `arXiv:math/0407171 [math.CO]`

[33] R. Pemantle and M.C. Wilson, *Asymptotics of multivariate sequences. I. Smooth points of the singular variety*, J. Combin. Theory Ser. A, **97**(1) (2002) 129–161; `arXiv:math/0003192 [math.CO]` *Asymptotics of multivariate sequences, II. Multiple points of the singular variety*, Combin. Probab. Comput. **13** (2004) 735–761. `arXiv:math/0406022 [math.CO]`

[34] R. Pemantle and M.C. Wilson. *Twenty combinatorial examples of asymptotics derived from multivariate generating functions*, SIAM Review, **50**(2) (2008)199–272. `arXiv:math/0512548 [math.CO]`

[35] R. Pemantle and M. C. Wilson. *Analytic Combinatorics in Several Variables*. Cambridge University Press, Cambridge, UK, (2013).

[36] D. Robbins and H. Rumsey, *Determinants and Alternating Sign Matrices*, Advances in Math. **62** (1986) 169–184.

[37] D. Speyer, *Perfect matchings and the octahedron recurrence*, J. Algebraic Comb. **25** No 3 (2007) 309–348. `arXiv:math/0402452 [math.CO]`.

Department of Mathematics, University of Illinois at Urbana-Champaign, MC-382, 1409 W Green St., Urbana, IL 61801, U.S.A. e-mail: philippe@illinois.edu

Department of Physics, University of Illinois at Urbana-Champaign, 1110 W. Green St., Urbana, IL 61801, U.S.A. e-mail: sotogar1@illinois.edu.